SILESIAN UNIVERSITY OF TECHNOLOGY

Faculty of Chemistry
Department of Organic Chemistry, Bioorganic Chemistry and Biotechnology

Tomasz Wasiak, MSc

Doctoral Dissertation

New generation of catalysts based on nanomaterials for advanced organic chemistry

Supervisor: Dr. Dawid Janas, prof. SUT

GLIWICE 2024

I would like to thank Dr. ***Dawid Janas,*** *prof. SUT for guiding and supporting my scientific career. Thank you also for your patience and motivating me to achieve my goals.*

I am grateful to be a member of the ***Functional Nanomaterials Group****, which is a team of wonderful personalities of young and outstanding scientists. I thank you for the unforgettable moments and the pleasant working atmosphere.*

I would also like to thank ***Dr. Pyry-Mikko Hannula, Prof. Mari Lundström, Prof. Ramesh Chandra,*** *and their research groups for their hospitality and the opportunity to participate in international collaborations.*

Finally, I would like to thank my family, who encouraged me to persist in my struggle and believed in me.

Abstract

Nanotechnology has revolutionized many aspects of modern science and industry. The discovery of unique properties of nano-sized particles resulted in numerous improved processes and applications. Thanks to quantum effects, well-developed surfaces, and almost endless possible compositions and morphologies, nanomaterials revealed new research opportunities. Among various nanomaterials, metal-based nanoparticles of different shapes are particularly interesting due to their hidden potential, which can be exploited in catalysis. Especially, anisotropic nanostructures like nanowires attract attention as their specific morphology enhances some of their properties.

As most chemical reactions used on a large scale are catalyzed by transition metals in bulk forms, it is expected that alternative solutions based on nanomaterials may provide even better performance. Lower noble metal load, higher activity, and better stability are key targets for scientists in this field. This work focuses on nanomaterial implementation to make highly efficient catalytic systems for organic chemistry transformations. During this research, nanowires were used as base structures for catalyst preparations. The conducted work includes their synthesis, characterization, application in nanocomposites with spherical nanoparticles of noble metals, and evaluation of their catalytic activity.

The dissertation is composed of a collection of monothematic articles, begins with a description of current knowledge about nanowires, their synthesis, and benefits and unresolved issues connected with nanowire application in catalysis. Then, an example of an ecological approach is presented that exploits industrial wastewater, rich in heavy metals, as a precursor of nanowires. Further parts of the thesis show the application of catalytic systems that utilize metallic nanowires and nanoparticles. Based on abundant non-noble metal nanowire structures decorated with highly active noble metal species, efficient catalysts were obtained and tested in advanced organic chemistry transformations.

Abstrakt

Nanotechnologia zrewolucjonizowała wiele aspektów współczesnej nauki i przemysłu. Odkrycie unikalnych właściwości nanocząstek zaowocowało wieloma udoskonalonymi procesami i aplikacjami. Dzięki efekom kwantowym, dobrze rozwiniętym powierzchniom oraz niemal nieograniczonymi wariantami składów i morfologii, nanomateriały otworzyły nowe możliwości badawcze. Spośród różnych nanomateriałów, bardzo interesujące są nanocząstki na bazie metali o rozmaitych kształtach, które to posiadają ukryty potencjał katalityczny. W szczególności anizotropowe nanostruktury, takie jak nanodruty, przykuwają uwagę naukowców ze względu na specyficzną morfologię, która wzmacnia niektóre z ich właściwości.

Jako że większość reakcji chemicznych stosowanych na dużą skalę jest katalizowana przez metale przejściowe w postaciach makroskopowych, przewiduje się, że alternatywne rozwiązania na bazie nanomateriałów mogą dać jeszcze lepsze osiągi. Niższa zawartość metali szlachetnych, poprawa aktywności i stabilności to kluczowe cele dla naukowców w tej dziedzinie. Niniejsza praca koncentruje się na wykorzystaniu nanomateriałów do konstrukcji wysokowydajnych układów katalitycznych dla przemian w chemii organicznej. W trakcie tych badań nanodruty wykorzystano jako główny materiał do syntezy katalizatorów. Prace objęły ich syntezę, charakterystykę, wytworzenie nanokompozytów ze sferycznymi nanocząstkami metali szlachetnych oraz analizę ich właściwości katalitycznych.

Rozprawę, złożoną ze zbioru monotematycznych artykułów, rozpoczyna opis aktualnej wiedzy na temat nanodrutów, metod ich syntezy oraz korzyści i nierozwiązanych problemów związanych z zastosowaniem nanodrutów w katalizie. Następnie przedstawiono przykład ekologicznego podejścia do zagadnienia tworzenia nanodrutów z ścieków przemysłowych bogatych w metale ciężkie. W dalszej części pracy przedstawiono zastosowanie układów katalitycznych wykorzystujących nanodruty i nanocząstki metaliczne. W oparciu o liczne struktury nanodrutów metali nieszlachetnych z osadzonymi wysoce aktywnymi nanocząstkami metali szlachetnych otrzymano wydajne katalizatory, które przetestowano w zaawansowanych przemianach chemii organicznej.

Glossary

CNTs	Carbon nanotubes
CPE	Conjugated polymer extraction
CV	Cyclic voltammetry
DFT	Density functional theory
DMFCs	Direct methanol fuel cells
ECSA	Electrochemically active surface area
EDA	Ethylenediamine
EDX	Energy-dispersive X-ray spectroscopy
HER	Hydrogen evolution reaction
HRTEM	High-resolution transmission electron microscopy
H-Si NWs	Hydrogen-terminated silicon nanowires
ICP-OES	Inductively coupled plasma optical emission spectrometry
MOR	Methanol electrooxidation reaction
NPs	Nanoparticles
NWs	Nanowires
OER	Oxygen evolution reaction
OLEDs	Organic light-emitting diodes
ORR	Oxygen reduction reaction
PFO	Poly(9,9-dioctylfluorenyl-2,7-diyl)
PFO-3DDT	Poly(9,9-dioctylfluorenyl-2,7-diyl-alt-3-dodecylthiophene-2,5-diyl
PL	Photoluminescence
PVP	Polyvinylpyrrolidone
RHE	Reversible hydrogen electrode
SAED	Selected area electron diffraction
SEM	Scanning electron microscopy
SM	Standard mode
SPS	Solid phase synthesis
STEM	Scanning transmission electron microscopy
SWCNT	Single-walled carbon nanotube
TEM	Transmission electron microscopy
TOF	Turnover frequency
TON	Turnover number
VLS	Vapor-liquid-solid
XPS	X-ray photoelectron spectroscopy
XRD	X-ray diffraction

The thesis is based on the following published articles:

[P1] T. Wasiak, D. Janas, Nanowires as a versatile catalytic platform for facilitating chemical transformations, J. Alloys Compd. 892 (2022) 162158.
https://doi.org/10.1016/j.jallcom.2021.162158

IF = 6.371, Ministerial points = 100

[P2] T. Wasiak, P.-M. Hannula, M. Lundström, D. Janas, Transformation of industrial wastewater into copper-nickel nanowire composites: straightforward recycling of heavy metals to obtain products of high added value, Sci. Rep. 10 (2020) 19190. https://doi.org/10.1038/s41598-020-76374-x

IF = 4.6, Ministerial points = 140

[P3] T. Wasiak, D. Łukowiec, S. Wacławek, J. Kubacki, D. Janas, Ni nanowires decorated with Pd nanoparticles as an efficient nanocatalytic system for Suzuki Coupling of anisole derivatives, Nano-Structures & Nano-Objects, 36 (2023) 101052.
https://doi.org/10.1016/j.nanoso.2023.101052

IF = - (not released yet), Ministerial points = 40

[P4] T. Wasiak, D. Just, A. Dzienia, D. Łukowiec, S. Wacławek, A. Mielańczyk, S. Kodan, A. Bansal, R. Chandra, D. Janas, PdNPs/NiNWs as a welding tool for the synthesis of polyfluorene derivatives by Suzuki polycondensation under microwave radiation, Sci. Rep. 14 (2024) 2336
https://doi.org/10.1038/s41598-024-52795-w
IF = 4.6, Ministerial points = 140

[P5] D. Łukowiec, **T. Wasiak**, D. Janas, E. Drzymała, J. Depciuch, T. Tarnawski, J. Kubacki, S. Wacławek, A. Radoń, Pd decorated Co–Ni nanowires as a highly efficient catalyst for direct ethanol fuel cells, Int. J. Hydrogen Energy, 47 (2021) 97.
https://doi.org/10.1016/j.ijhydene.2021.11.177

IF = 7.2, Ministerial points = 140

Total IF = 22.771 Total Ministerial points = 560

Table of Contents

1. Introduction

The thesis consists of the following parts: Introduction, Aims and scope of the work, Results and discussion, Conclusions and further perspective. The first section contains basic information about nanomaterials and the state of their development. As my work focuses on metallic nanoparticles, particularly nanowire-like nanostructures, their synthesis and applications are presented first. Next, in the Aims and scope of the work, I outline the key objectives and perspectives of the dissertation. The subsequent main part of this thesis includes the obtained results and their discussion based on scientific papers published in research journals. Each subsection references to specific topic of nanowire synthesis, formation of composite materials and gauging of their catalytic properties in various chemical and electrochemical reactions. The last section underlines conclusions obtained from the described works and presents future opportunities for the investigated topic.

1.1. Nanotechnology – great potential in small things

Nanotechnology deals with the synthesis, structure, size modification and application of nano-size objects in the range 1-100 nm in at least one dimension. Quantum effects present in those entities provide improved characteristics such as higher surface area and reactivity or better optical/electrical properties. The development of nanotechnology, which converts nanoscience theoretical values to applicable forms, gave bountiful opportunities to improve many aspects of various fields such as chemistry, biology, medicine or electronics [1]. In 1959 the concept of nanotechnology was introduced by an American physicist Richard Feynman, who presented a lecture at the annual meeting of the American Physical Society entitled “There’s Plenty of Room at the Bottom”. He postulated that Encyclopaedia Britannica could fit on the head of a pin and talked about creating materials on the molecular level [2]. In 1974, nanotechnology was defined by Norio Taniguchi. According to him, “nanotechnology mainly consists of the processing of separation, consolidation, and deformation of materials by one atom or one molecule” [3]. The discovery of carbon nanotubes (CNTs) by Iijima and Ichihashi in 1991 was a huge step in the development of nanotechnology

[4,5]. Scientists gained awareness of possible beneficial properties hidden in nanomaterials and thus started to research this subject on a larger scale. Some focused on nanostructures similar to CNTs, however, with less handling and manufacturing issues. Nanowires (NWs) are anisotropic nanostructures built from various materials such as metals [6–8] non-metals [9], and their compounds with other elements [10–12]. In the samples from the XVI century, scientists discovered that ore deposits contained very thin single crystals built only from metal atoms, which were called whiskers. In the mid-XX century, Bell Telephone Laboratories studied the formation of thin materials from Al_2O_3 and SiC. The superior strength of up to 10^{10} Pa obtained for micron-size particles encouraged scientists to continue research of additives of reduced size for alloys and plastics. Silicon whiskers produced by the Vapor-liquid-solid (VLS) mechanism by Wagner accelerated the development of such materials [13]. Structures based on Al_2O_3, GaP, MgO or NiO were obtained as thin crystals. Further studies of synthesis parameters revealed the possibility to fabricate Si-based nanostructures with diameters of 10 nm [14]. In 2001, Transmission Electron Microscopy (TEM) allowed an in situ study of the VLS process, which provided essential information about nanowire growth and confirmed Wagner's mechanism. Due to the work of many scientific groups, nanowire research soon transformed into an interdisciplinary field, connecting chemists, physicists, and material scientists to discover new nanomaterials and their unique properties. This resulted in a bountiful variety of nanowires with different compositions. The main efforts of those works were addressed to synthesis methods and application of nanowires in various key aspects of modern science and technology. The work described herein focuses on the catalytic properties of nanowire-based nanomaterials and therefore in the following paragraphs, the synthesis of such composites and their application in catalysis will be discussed.

1.2. Nanowire synthesis

In [P1], I conducted a literature study of nanowire synthesis and their application in catalysis. The most characteristic feature of nanowires is their anisotropic morphology, which provides beneficial properties that come from enhanced quantum effects.

Formation of such structures can be achieved by two distinctive approaches. Top-down methods include techniques allowing selective removal of atoms from bulk substrate. Precise control over orientation and size of nanostructure leads to fabrication of high-quality nanowires with small defects count. For that purpose, lithography gained attention due to high resolution of 0.1 nm [15–18]. Multiple variants of that method are commonly used like electron beam lithography [19], nanoimprint lithography [20,21] or stencil lithography [22]. Those techniques showed particular utility in microelectronics industry due to ability to fabricate semiconducting nanowires. As a substrate i.e. wafer is etched from excess material, etch mask protects remaining atoms, therefore anisotropic pattern is achieved (Fig. 1). Nanowires obtained in this way tend to exhibit tapered morphology due to unintended etching underneath the mask [23]. The main benefit of lithography is ability to produce highly ordered nanowire arrays, which find application in microelectronics. However, several drawbacks like expensive and complex equipment, difficult composition manipulation and sophisticated scale-up procedures, decrease the large-scale application potential of this method.

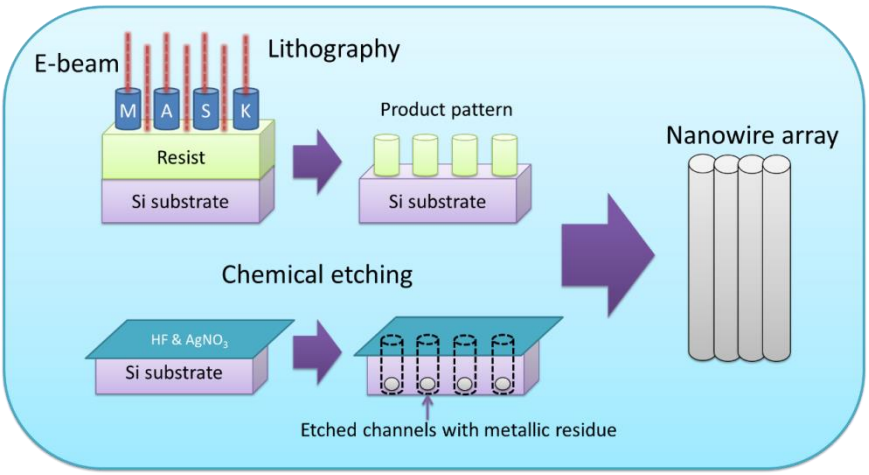

Fig. 1. Schematic illustration of methods of synthesis of nanostructure materials based on top-down approach.

A far more convenient alternative to top-down methods comes from bottom-up processes, where nanomaterials are built block-by-block from molecules. This approach utilizes chemical reactions, which provide the growth of nanoparticles (NPs) in a controlled manner due to the selection of conditions and additives. The most

common techniques in this category involve reactions in gas and liquid phases. Already mentioned VLS method (Fig. 2) proved its usefulness in the formation of numerous NWs made from ZnS [24], SnO_2 [25], In_2O_3 [26], Fe_2O_3 [27], and Si [28]. In such syntheses, inert gas transports compounds in gaseous form or as solutions, along the tube furnace filled with deposited catalyst. Catalyst supersaturated with precursor releases atoms, and thus crystallization of metal clusters occurs, which contributes to the thermally-driven growth of nanostructures. Simplicity and a wide diversity of precursors and substrates are the main advantages of such a method. Versatility in forms of products (powders, films) is also worth mentioning.

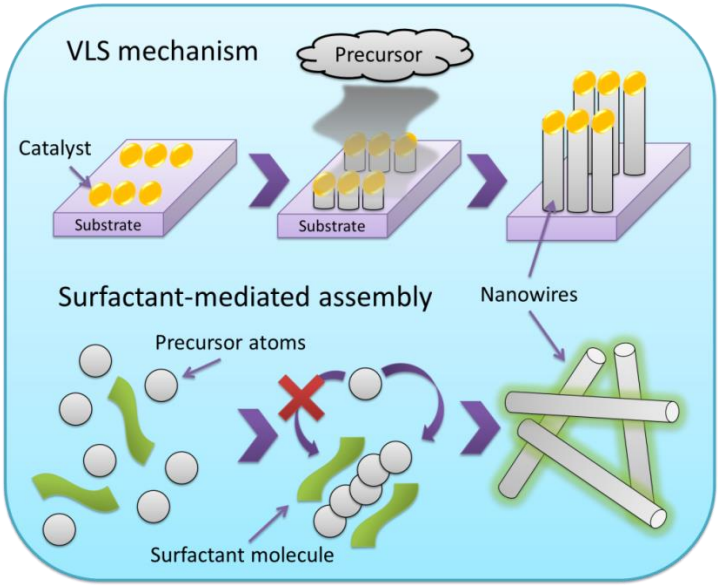

Fig. 2. Schematic illustration of methods of synthesis of nanostructure materials based on bottom-up approach.

Solution-based methods refer to techniques incorporating nanowire growth in solutions containing metal ions. This type of synthesis gained attention due to superior results for the fabrication of high-quality NWs with easy scale-up possibilities. Explored chemical routes allowed the preparation of metallic and semiconducting NWs. Although some procedures seem to enrol harsh conditions like Heath's synthesis of germanium NWs [29], outcomes justify such conditions. Along with his team, Heath used metallic sodium dispersion in toluene to reduce $GeCl_4$ and phenyl $GeCl_3$ in dry hexane at elevated temperature and pressure. Obtained nanostructures exhibited diameters in the range of 7-30 nm and lengths up to 10 µm. The solvothermal methodology was

exploited for other nanowires made of cobalt [30], zinc oxide [31], cadmium sulfide [32], or silver [33,34]. Simple solution and one-pot methods are most attractive for industrial use due to mild conditions in comparison to gaseous phase approaches [35]. By controlling reaction parameters such as concentration, temperature, time, solvent, additives, and pH, obtained nanowires can be very homogeneous in terms of diameters and length. Furthermore, the reaction atmosphere can be easily tuned by the introduction of inert gas, which prevents undesired oxidation of NWs [36].

Reduction of metal ions is a common strategy to obtain NWs. It can be enhanced by surfactants, which promote anisotropic growth (Fig. 2). They act as capping agents, adsorbing on specific crystallographic faces and blocking additional atoms from being built into the forming nanostructure. According to Wulff's theory, it is done by modification of facets free energies, which have an impact on the overall shape of growing crystal [37]. Good shape control, formation of highly crystalline products, and easily scalable processes are key aspects of solution-driven synthesis of nanowires. A lot of work is dedicated to transition metals in this regard. Nickel [38–40], copper [41–44], cobalt [45,46], and silver [7,47] are only a few examples of possible solution-based synthesis outcomes.

Template-assisted methods can also promote the anisotropic growth in solution-based approach. During such procedures, a template acts as scaffolding for nanowire growth on or inside selected spaces. The main parameters, that influence the reaction, are pore size and their uniformity. Macroscopic features of templates such as thickness and chemical composition are also vital points of successful synthesis, due to post-treatment steps involving template removal. Two characteristic groups of templates can be distinguished: hard and soft. Anodic aluminum oxide [48], zeolites [49], and track-etched polycarbonate [50] represent the former, whereas polymers [51], DNA [52], micelles [53], and gels [54] are examples of the latter. Filling the pores is crucial for uniform NWs, which can be achieved by applying vacuum suction, pressure, or by full template immersion in the solution. Unfortunately, using hard templates generates smaller yields in comparison to soft templates. To a further extent, template-assisted growth can be combined with electrochemical techniques, which can improve control over the morphology of forming nanostructures to produce nanowires, nanorods, or even

nanotubes as homo- and heterostructures with various compositions [55]. Diffusion of metal ions from solution to pores is therefore enhanced by the external field and the reduction occurs inside the template attached to the cathode. Varying the parameters of electric current, electrodeposition modes, and reaction time, the size of growing NWs can be controlled [56]. Besides the multiple conditions and potential variables, which have to be addressed properly, electrodeposition was successfully utilized to obtain a bountiful collection of nanowires, including those made of Co [57], Cu [58], Ge [59], Pt [60], ZnO [61], Co-SiO_2 [62], BiTeSe [63].

Another interesting way of nanowire synthesis is electrospinning, which allows the formation of different nanostructures and compositions such as porous or core-shell NWs [64,65]. This process involves conducting polymer solution containing metal salt, which is then ejected through the metal needle, connected to high-voltage power. An electric field deforms the droplet into a cone-like jet stream, which follows the grounded collector. Solvent evaporation results in solidified nanofibers appearing on the collector. Such process is highly cost-effective, versatile, and can be easily scaled up to meet industrial demands. However, size control of formed NWs is challenging due to numerous parameters, which must be precisely estimated and maintained. Furthermore, environmental conditions such as temperature or humidity can hinder the results of electrospinning [65].

As indicated in the above discussion, the synthesis of nanowires can be conducted in various ways. The synthetic methodology is dictated by desired outcome, which consists of process scalability and properties of designed nanowires. Each approach has several advantages and may be exploited for specific elements; however, drawbacks are their inherent parts. To this day, an ecological, cost-effective, and universal method for large-scale fabrication of nanowires has not been developed, which only encourages scientists to continue their studies. Most of the presented approaches are believed to be great opportunities for the implementation of nanowires in industry and large-scale applications, however, they need major improvements to be considered profitable and safe for the environment and people. This summarizes the NW synthesis paragraph of this work. The next part focuses on the application of nanowires in catalysis, which is the clou of the presented thesis.

1.3. Nanowires application in catalysis

Catalysis is a topic of high priority due to the widespread of catalyst-driven reactions across the entire chemical industry. From basic one-step transformations to complex synthetic routes, catalysts are key ingredients during the development of various chemical compounds produced on a large scale. As they accelerate certain reactions, or even enable their progression, their vital role is underlined in many reviews [66–72]. Their common property is lowering the activation energy; however, their mechanisms may vary due to their composition, morphology, and working conditions. Catalysis can be divided into two different approaches, defined by the phase character of the catalyst concerning the reaction environment. Homogeneous catalysis occurs when catalysts and reactants are present in the same phase. In contrast, heterogeneous variants require the separation of both individuals between two phases. The most commonly used category in industry is homogeneous catalysis. It often exhibits higher activities, yields, and therefore better turnover numbers (TON) and frequencies (TOF), which are the most important industrial parameters. Furthermore, homogeneous catalysts tend to be more selective towards desired products and can be characterized at ease, even by mechanistic studies. Despite such great advantages, they show some drawbacks, which have been targets of scientists for a long time. The catalyst is sometimes irrecoverable from the post-reaction mixture. This is a challenging issue, especially for drug synthesis, where highly toxic complex-based catalysts are used. Overall, homogeneous catalysis involves additional steps during the main process, which can generate higher costs and hazards, which results in lower profits.

Such unfavorable quirks of homogeneous catalysis are absent when using heterogeneous counterparts. Heavy industries, like petrochemical, and gas processing, especially in continuous reactions, rely on heterogeneous catalysts, which although have lower activities, they can be recycled conveniently. This crucial advantage over homogeneous catalysis resulted in increased efforts directed toward the development of highly active and stable heterogeneous catalysts. Additional benefits such as greener ecological approaches for catalysts preparations, heavy metals utilization, and better resource management, were the main driving forces of study in this matter.

Even more emphasis in this regard is put on nanostructures, due to their unique properties and potential opportunities. A plentiful range of nanomaterials with various morphologies and compositions still wait to be discovered and tested as catalysts in numerous reactions. One such promising category is metal-based one-dimensional nanomaterials, such as nanowires, which proved to be an interesting emerging field for catalysis. They can be formed by various methods, which were discussed in the previous part of the presented dissertation. As the spectrum of potential applications is very wide and rich in examples, this work only summarizes key burning issues, which are addressed by the largest scientific groups of interest. Further discussion involves the state of nanowire application in coupling reactions, reduction, electrocatalysis, and photocatalysis (Fig. 3).

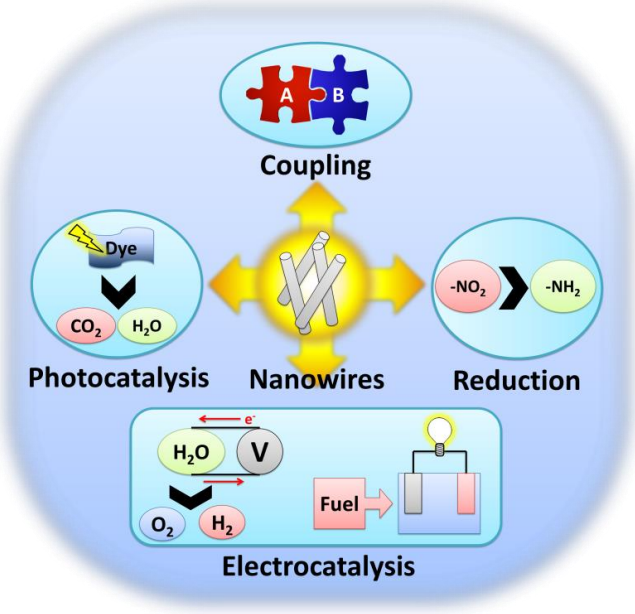

Fig. 3. Application of NWs as catalysts.

1.3.1. Coupling reactions

Joining smaller compounds into more advanced structures is commonly used across syntheses of pharmaceuticals [73,74], agriculture chemicals [75,76], and polymers [77,78]. The formation of C-C or C-heteroatom bonds is highly important as it leads to many building blocks for the aforementioned substances. Through decades, Ullmann's reaction[79,80] was modified and applied by other eminent researchers, which resulted in

a group of coupling reactions such as Suzuki [81], Kumada [82], Stille [83], Negishi [84], Sonogashira [85], and Heck [86]. Their design allows coupling of specific nucleophiles with electrophilic substrates. Whereas first coupling attempts were driven by copper-based catalysis, further studies showed the superiority of nickel and palladium in this topic, which shaped the current state of modern application [79,87]. Other elements also proved to be useful. Organometallic complexes based on tin [83], zinc [88], magnesium [82], or boron [81], allowed efficient coupling of more advanced systems. However, their catalytic performance comes with some setbacks like the highly toxic components needed for the synthesis of complex catalysts, which is a serious environmental issue. Expensive palladium challenges scientists to improve catalysis in every possible way to gain the most benefits. Others search for alternatives, whose production will be less harmful to ecosystems and wallets of potential industrial clients. In terms of nanowires, they are believed to solve many problems generated by coupling reactions.

Suzuki-Miyaura reaction is commonly used as a testing ground for new coupling reaction catalysts. Easy-accessible aryl halides and arylboronic acids are joined together with the assistance of metal atoms (Fig. 4). Nanoparticles, especially spherical ones, are studied the most in the Suzuki reaction. However, some experiments showed even more significant improvement in catalytic properties when nanowires were applied. Chawla et al. exploited Pd NWs, which exhibited better results than spherical nanoparticles [89]. Nanostructure synthesis involved co-surfactants, which enabled the formation of hexagonal mesophases, which acted as soft templates. Followed by controlled decomposition of bis-benzylidene acetone Palladium (0) in a hydrogen atmosphere, palladium nanowires were obtained. 20 times lower catalyst loads were needed to reach similar conversions as for the usage of NPs. Such outcomes revealed hidden opportunities for NW-driven reactions.

Other research groups focused on reducing Pd content in catalytic nanomaterial. Lv fabricated Pd-Cu bimetallic NWs, whose synergistic effects of both metals and unique morphology resulted in quantitative yields, high selectivity, and stability. The presented nanocatalyst was able to promote reaction even for chlorobenzenes, whose low reactivity is a common issue. Notable results were also achieved by Lakshminarayana, who used combustion synthesis for $CuFe_2O_4$ and then reduction of

$PdCl_2$ with $NaBH_4$ to obtain Pd/$CuFe_2O_4$ NWs [90]. Such nanostructure was able to achieve 98% yields for 4-methoxybiphenyl synthesis for just 10 minutes of reaction. Interesting, this catalytic system proved to be compatible with moieties like –NO_2, –F, or –Cl, enabling reaching a wide spectrum of derivatives. High stability and consistent conversion over several recycles strongly underline the benefits of a heterogeneous catalytic system.

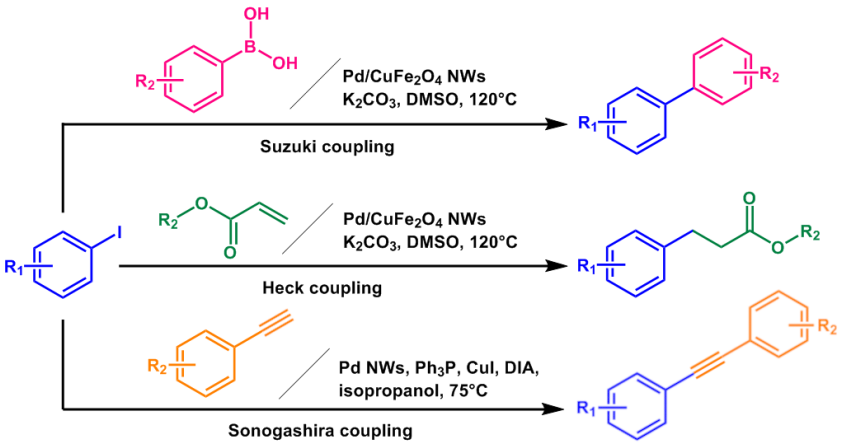

Fig. 4. Synthesis of biphenyls by Suzuki cross-coupling [90], alkyl cinnamates by Heck cross-coupling [91], and aromatic alkynes by Sonogashira cross-coupling [92]. Reproduced with permission from [93]. Copyright (2022) Elsevier.

Pd/$CuFe_2O_4$ NWs also promoted the Heck reaction, which focuses on substrates containing double bonds (Fig. 4) [91]. As target products, researchers chose cinnamic acid esters and stilbenes, whose syntheses exceeded 90% yields. The main advantage is simplifying the production of those compounds, by reducing the two-step Claisen-Schmidt condensation and hydrogenation method to a one-pot procedure. Even dihydrochalcones, known for their antifungal and anticancer properties, could be obtained by the Jeffery-Heck reaction.

Another C-C bond formation method is Sonogashira coupling (Fig. 4) [85]. Terminal acetylenes were coupled with aryl halides by branched Pd NWs [92]. The seeded growth of nanowires was possible due to ion liquid-stabilized gold nanoparticles. Gao and co-workers showed 100% conversion, which lasted almost unchanged for four catalytic cycles (Table 1). C-heteroatom bond formation was also studied in a matter of nanowires-catalyzed coupling reactions. A core-shell nanowires like Cu@Cu_2O NWs are

a perfect example [94]. As copper foam was oxidized and passivized, highly ordered arrays of NWs were formed. They exhibited significant performance of 80-99% yields in coupling aryl iodides with modified thiols under mild and ligand-free conditions (Table 1).

C-N bonds were also investigated due to being a vital point in the production of pharmaceuticals and agrochemicals. Nasrollahzadeh's team proposed Pd/Fe_3O_4 NWs as an alternative catalyst for the synthesis of monoarylureas [95]. Fast and convenient preparation of magnetic and eco-friendly catalytic system was done by arc discharge in water, followed by drop-drying of Pd-containing solution. Such a heterogeneous system achieved promising results for ligand-free amidation and therefore, the challenging synthesis of N-monosubstituted ureas was resolved, which was proven by reaching almost 90% yields. True catalytic centers of the catalyst were generated by the formation of Pd nanoparticles, decorating NWs during the reaction. The postulated mechanism involved C=N intermediate, intramolecular water elimination, and double-bond hydrogenation. In another study based on Pt NWs, Hu et al. proposed an intramolecular direct dehydration mechanism [96]. Once again nanowires proved their catalytic properties and high yields were obtained. Tests also included a greener approach, by utilizing water as solvent with 88% of N-benzylbenzeneamine yield. The aforementioned examples of nanowire application in coupling reactions are listed in the table below.

Table 1. Comparison of properties of NW-based catalysts in various coupling reactions. Reproduced with permission from [93]. Copyright (2022) Elsevier.

Catalyst	Coupling reaction	Solvent	Temp. [°C]	Time [h]	Yield [%]	Product	Ref.
Pd NWs	Suzuki	Toluene	90	9	80	Biphenyl	[89]
Pd/Cu NWs	Suzuki	DMF/H_2O	80	2	99	Biphenyl	[97]
Pd/$CuFe_2O_4$ NWs	Suzuki	DMSO	120	12	91	Biphenyl	[90]
Pd/$CuFe_2O_4$ NWs	Heck	DMSO	120	24	64 - 86	DHCs	[91]
Pd NWs/IL	Sonogashira	Isopropanol	75	7 -10	100	Diphenylacetylene	[92]
Cu@Cu_2O NWs	C-S	DMSO	110	12	99	Octyl (4-methylphenyl) sulfide	[94]
Pd/Fe_3O_4 NWs	C-N	MeOH	120	1	87	1-Phenylurea	[95]
Pt NWs	C-N	Toluene	100	24	94	N-phenyl-4-methoxybenzylamine	[96]

1.3.2. Reduction reactions

Reduction of various chemical functional groups is a commonly used procedure. Nitroaromatic compounds are dealt with significant emphasis. A lot of industrial and agricultural wastewater contains high concentrations of such hazardous substances, which generate crucial threats to the environment. A common method to transform such compounds into a more convenient state is catalyzed reduction by $NaBH_4$ [98].

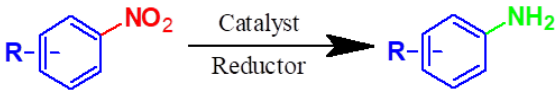

(1)

To test new systems, 4-nitrophenol is often selected by scientists (Reaction 1). In this field, nanowires showed promising results. Starting with Pd-based NWs, their excellent performance surpassed nanoparticles [99]. Furthermore, alloying with nickel improved catalytic activity 7.7 times. This can be explained by better adsorption of substrate on nickel atoms. In this case, nanowire anisotropic growth was enhanced by amidoamine derivative with amphiphilic properties, which resulted in 3.5±0.4 nm diameters, enhancing the catalytic activity of the system. Similar outcomes can be seen in Chawala's work [89], where diameters of 5±0.9 nm were observed. Additionally, surfactants used for obtaining mesophases remained on the surfaces of nanowires, which protected them against poisoning and improved the adsorption of reactants. To decrease costs, other more accessible elements were incorporated in studies of nanowire-based reduction catalysis.

Copper is an example of such an abundant and cheap alternative to noble metals like palladium. An interesting nanostructure was achieved by the reduction of Cu^{+} and Cu^{2+} ions with ascorbic acid, in the presence of cetyltrimethylammonium chloride [100]. Nanowires with highly rough surfaces exhibited enlarged surface area and therefore better catalytic activity towards the reduction of nitro compounds. Another approach to enhancing Cu NWs reactivity was decoration with silver atoms by galvanic replacement, which improved catalytic properties even further.

Some scientists focused on nickel insertions into Cu NWs [101]. The synergy between both metals, along with high surface area resulted in a significant rise of reactivity in comparison to bare Ni NWs. Scientists postulated that the increased number of

available corners and edges were sources of those improvements. To push numbers even higher, Ni/Cu NWs were supported by graphene, which enabled electron migration from the NW surface and thus made it more electrophilic [102]. This facilitated the adsorption of reductive agent (BH_4^-) and 4-nitrophenolate ions on the NW surface and thus accelerated reduction. Another bimetallic composition worth mentioning is prickly Ni NWs which were shelled with silver [103] and gold [104]. The former was obtained by $NiCl_2$ reduction in a mixture containing Tollens' reagent ($Ag(NH_3)_2OH$). The latter was based on a two-step process involving Ni NWs fabrication, followed by $HAuCl_4$ solution treatment. Both of them, unfortunately, resulted in lower catalytic activities in comparison to Cu-based systems (Table 2). As Fu et al. discovered, Ag/Au NWs performed better than Ni@Ag and Ni@Au NWs [105]. In summary, the discussed examples revealed that Cu and Pd are the most promising candidates for nanowire-driven catalysis of 4-nitrophenol reduction.

Table 2. Comparison of catalytic properties of NW-based catalysts in the reduction of 4-nitrophenol. Reproduced with permission from [93]. Copyright (2022) Elsevier.

Catalyst	Rate constant k_a (min^{-1})	Activity factor K ($mg^{-1} \cdot min^{-1}$)	Ref.
Pd/Ni NWs	1.00	/	[99]
Surfactant-protected Pd NWs	2750	/	[89]
Cu NWs	0.25	/	[100]
Cu NWs/Ag	0.40	4.44	[100]
Cu/Ni NWs/graphene	1.16	5.81	[102]
Ni/Cu NWs	0.91	0.057	[101]
Ni/Ag core-shell NWs	0.13	0.26	[103]
Ni/Au core-shell NWs	0.08	0.01	[104]
Ag/Au NWs	0.23	0.91	[105]

1.3.3. Electrocatalysis

Besides reactions driven by chemical potentials, electricity is another form of energy, which can be utilized to conduct chemical transformations. Nonetheless, electrochemical processes are challenging. Electrocatalysts have to be precisely designed to withstand continuous redox reactions for a prolonged time and exhibit stable high activities. Nanomaterials could resolve such problems, like metal nanoparticles supported on conductive materials. A carbon cloth can be an example, which improves electric current flow to actual electrocatalytic sites, however, such

systems tend to corrode and leach, which drastically decreases their catalytic performance [106,107]. More advanced nanostructures such as nanowires with anisotropic morphology may minimize those issues. Their main advantage is very high surface area and conductivity [108]. Lack of occurring coalescence, as opposed to nanoparticles, also promotes higher catalytic activity [109]. There are numerous electrocatalytic reactions, but not all of them include nanowires as a part of catalytic systems. Here only the most important processes are discussed. Starting with water splitting, which can provide eco-friendly and renewable hydrogen sources, which gathered attention of many research groups [110,111]. The process consists of a hydrogen evolution reaction (HER) (Reactions 2, 4), which occurs on the cathode, and an oxygen evolution reaction (OER) (Reactions 3, 5) which occurs on the anode (Fig. 5). In acidic medium half-cell reactions occur as follow:

$$\boldsymbol{2H^+ + 2e^- \rightarrow H_2} \qquad \textbf{(2)}$$

$$H_2O \rightarrow \frac{1}{2}O_2 + 2H^+ + 2e^- \qquad \textbf{(3)}$$

Whereas, in alkaline medium water electrolysis process in different manner:

$$2H_2O + 2e^- \rightarrow H_2 + 2OH^- \qquad \textbf{(4)}$$

$$2OH^- \rightarrow \frac{1}{2}O_2 + H_2O + 2e^- \qquad \textbf{(5)}$$

For sustainable production of those gases, highly active and state-of-the-art catalysts have to be used. Nowadays, the most common choice is Pt-based anodes and Ir or Ru-based cathodes [112]. Due to the high prices of those elements and their low abundance, overall profitability is limited. Many studies postulated that nanowires could be desired nanomaterials for that application. Ultrathin 2 nm wide Pt NWs accompanied with single-layered 2D nickel hydroxide nanosheets showed even five times increased catalytic activity for HER reaction compared with commercial Pt/C catalyst [113].

Alloyed Pt NWs were also successive in this matter. $Fe_{56}Pt_{44}$ NWs prepared by Gue et al. from $Fe(CO)_5$ and $Pt(acac)_2$ were only 2.5 nm thick [114], while acetic acid activation allowed for surpassing 3.2 nm Pt catalyst in oxygen reduction reaction (ORR). More complex morphologies such as zigzag-like Pt_3Fe NWs supported by carbon black also showed better performance in comparison to commercial material [115]. Even higher values were observed for PtNiCo NWs [116]. Heterostructures were also investigated. Metal-sulfide junctions with dense interfaces and specific electronic and surface characteristics could improve catalysis even further. Pt_3Ni/NiS NWs are perfect examples, as they exhibited spectacular mass activity of 37.2 mA cm^{-2} for HER [117] (Table 3).

The core-shell approach of Koenigsmann's group achieved 1.83 A/mg of mass-specific activity for Pt/Pd NWs [118]. This study shows that lowering Pt load can be done with NWs. Another pathway to better catalytic systems leads through non-noble metals, which can be easily converted into nanoscale anisotropic materials. CoP NWs/CoMoP nanosheets exhibited high HER activity due to synergy between their ingredients [119]. As CoMoP enhanced the dissociation of H_2O, the CoP NWs allowed better adsorption of hydrogen, and thus improved properties were observed. Another interesting finding was presented by Yang, which used amalgamated Co and Mo as Co-N-MoO_2 NWs with bountiful active sites [120]. The formed bifunctional nanocatalyst was able to reach 69 mV of overpotential vs reversible hydrogen electrode (RHE).

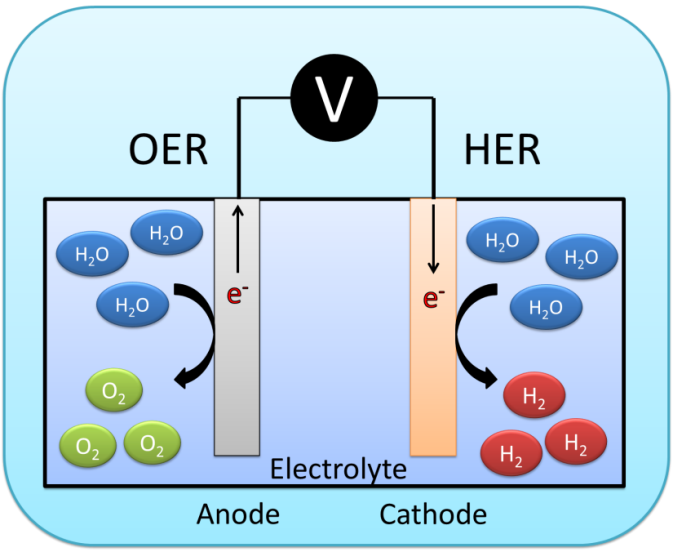

Fig. 5. Scheme of electrocatalytic water oxidation.

Other metals like manganese are also considered due to their high abundance and minor toxicity. MnO_2 NWs were exploited in composite material by adding nickel and 1,3,4-thiadiazole-2,5-dithiol [121]. Such a system could work under the same potential as a RuO_2 catalyst (1.492 V vs. RHE). As the ruthenium price has blown sky-high in 2021, this solution lowered costs drastically. However, the importance of expensive and more reactive metals was also explored.

Iridium in the form of wavy NWs showed outstanding performance for OER and HER due to the developed surface area and therefore higher catalytic activity [122]. Alloying iridium with nickel or cobalt showed that a compromise between price and activity could be possible [123], although it requires better optimization for large-scale usage. Metal oxides were also utilized for OER electrocatalysts. Fe-TiO_x NWs/Ti properties observed by Zhao et al. were reasonable for application, as they operated at 0.26 V overpotential vs. RHE exhibiting 1 mA cm^{-2} current density [124] (Table 3). Metal nitrides like CoN NWs with large lattice spacing showed even higher values of 10 mA cm^{-2} at 0.29 V [125] (Table 3). Non-noble metals attracted the attention of many research teams in this matter as well. The most obvious choice was copper, whose very high abundance, low price, high conductivity, and convenient handling made it a perfect candidate for a versatile catalytic platform. An interesting implementation could be a core-shell 3D nanocomposite of Cu/NiFe NWs, whose layered double hydroxide structure exhibited very promising results [109]. Accelerated electron transport by developed surface and improved gas release were key features of such a system. The current density of even 100 mA cm^{-2} at 1.69 V surpassed values generated by IrO_2(+)//Pt(-) catalysts and lowered costs. Nickel-based NWs like NiSe [126] and NiS_2 [127] also showed promising outcomes. The high stability of nickel and cost-efficient production are major advantages of those nanocatalysts. This proved the concept of noble-metal-free catalysts, which can achieve high activities at lower prices.

Table 3. Comparison of catalytic properties of NW-based catalysts in water-splitting. Reproduced with permission from [93]. Copyright (2022) Elsevier.

Catalyst	ECSA [$m^2 g^{-1}$]	Electrolyte	η [V] vs. RHE	Current density [mA cm^{-2}]	Tafel slope [mV dec^{-1}]	Ref.
Pt NWs/SL-Ni(OH)$_2$	22.8	0.1 M KOH	0.058	4	/	113
$Fe_{56}Pt_{44}$/C	/	0.1 M $HClO_4$	0.9	3.9	/	128
Pt-skin Pt_3Fe z-NWs/C	34	0.1 M $HClO_4$	0.9	4.34	76	115
PtNiCo NWs	82.2	0.1 M $HClO_4$	0.9	5.11	/	116
Pt_3Ni_2 NWs-S/C	/	1 M KOH	0.070	37.2	/	117
Pt monolayer/Pd NWs	/	0.1 M $HClO_4$	0.9	0.77	/	129
CoP NWs/CoMoP	4.67	1 M KOH	0.034	10	33	119
Co-N-MoO_2 NWs	31.97	0.1 M KOH	0.258	10	126.8	120
Ni/DMTD/MnO_2 NWs	32.89	1 M KOH	0.262	10	69.46	121
Ir NWs	31.3	0.1 M $HClO_4$	0.283	10	47	122
Ir/Ni NWs	70	/	/	/	/	123
Ir/Co NWs	40	/	/	/	/	123
Fe/TiO_x NWs/Ti	/	0.5 M H_2SO_4	0.260	1	126.2	124
CoN NWs	/	1 M KOH	0.290	10	70	125
Cu/NiFe NWs	/	1 M KOH	0.116	10	58.9	130
NiSe NWs	/	1 M KOH	0.096	10	120	126
NiS_2 NWs	/	1 M KOH	0.165	10	94.5	127

Another electrocatalytic reaction, whose development is crucial for industry, is electrooxidation. Among many suitable substrates, alcohols emerged as convenient power sources. Methanol electrooxidation reaction (MOR) is particularly important, due to the promising results of direct methanol fuel cells (DMFCs) (Fig. 6) [131].

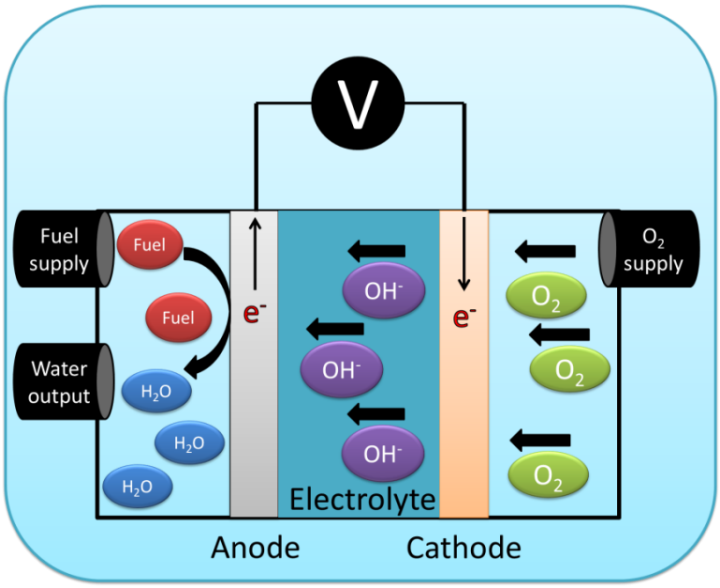

Fig. 6. Scheme of anion exchange membrane fuel cell.

Currently, the best commercial catalysts for MOR are Pt-based bulk structures. However, nanostructures can provide necessary improvements for more profitable applications. Highly ordered nanoporous Pt NWs, prepared by a dual-template approach, are perfect examples of how quantum effects and developed surfaces

exhibited by nanowires may implement those changes. Zhang et al. observed that smaller mesopore size in the template allowed for obtaining thinner NWs, which had higher electrochemically active surface area (ECSA) reaching 40.2 $m^2 g^{-1}$.

Core-shelling and alloying of various metals could benefit certain electronic characteristics and reduce the costs of the overall nanocatalyst. Wang proposed Pd/Pt NWs arrays, obtained by electrodeposition of Pd NWs, followed by sputtering of Pt thin coating [132]. The synergistic effect provided by specific morphology gave promising results in the form of more negative peak potential and higher current density. PtPdTe NWs [133] and PdRuPt NWs [134] exhibited similar values. Guo et al. showed that catalytic properties strictly depend on alloy composition [135]. They used FePtPd NWs as an example, in which Pd concentration controlled the shift of peak potential. Further studies revealed that multi-shell nanowires can achieve even more spectacular results. Pt_5FePd_2 NWs gave 4.038 A mg^{-1} mass activity (Table 4), and after multiple electrocatalytic cycles, their morphology was untouched [136]. Other three-metallic systems were also exploited. The palladium-free approach was presented by Li, whose PtFeNi NWs were composed of ionic liquid to promote reaction in proton exchange membrane fuel cells [137]. Many more nanowire-based electrocatalysts were prepared recently, however, most of them are still under development due to technological issues and immaturity of concepts.

Table 4. Comparison of catalytic properties of NW-based catalysts in methanol electrooxidation. Reproduced with permission from [93]. Copyright (2022) Elsevier.

Catalyst	Mass activity [mA mg^{-1} (M)]	Specific activity [mA cm^{-2}]	CO oxidation peak potentials	Ref.
Nanoporous Pt NWs	398 (Pt)	0.98	/	[138]
Pd/Pt NWs	756.7 (Pt)	22.7	0.54 V vs. SCE	[132]
PtPdTe NWs	595 (Pt)	/	/	[133]
$Pd_{0.97}Ru_{0.44}Pt$ NWs	1100 (Pt)	1.98	/	[134]
$Fe_{28}Pt_{38}Pd_{34}$	488.7 (Pt)	/	/	[139]
Pt_5FePd_2 NWs	4038 (Pt)	/	/	[136]
PtFeNi NWs	750 (Pt)	0.86	/	[137]
PtFeNi NWs/ionic liquid	1430 (Pt)	1.64	/	[137]
Pt/Zn NWs	1005.3 (Pt)	3.48	0.581 V vs. SCE	[140]
$PtCu_2$ NWs	1287 (Pt)	1.87	0.478 V vs. SCE	[141]
$Cu(OH)_2@CoCO_3(OH)_2 \cdot nH_2O$ NW/CF	/	0.223	0.5 V vs. SCE	[142]

1.3.4. Photocatalysis

Since Fujishima showed photoinduced water decomposition on TiO_2, a lot of emphasis is put on the development of photocatalytically active materials [143]. Those efforts are motivated by new opportunities for resolving energy shortage and organic pollutants issues [144–146]. Visible light generated by the Sun is virtually infinite (for our generation) and can enable chemical transformations, which are limited by ambient conditions.

Common examples of how new photocatalysts can be tested involve degradation of organic dyes (Fig. 7). Wastewater produced by the textile industry is often polluted with numerous dyes, which is a burning issue for the environment. Photocatalytic degradation of such compounds may solve the problem, which other methods like membrane processes and activated carbon adsorption struggle to overcome [147–149]. Nanowires, especially of semiconductor type, exhibited particularly valuable contributions to this issue, out of which a few examples can be seen in Table 5.

Hydrogen-terminated silicon nanowires (H-Si NWs) successfully degraded methylene blue and methyl orange [150] (Table 5). Brahiti proposed mechanism was based on electron-hole pair generation on the surface of NWs. Photoelectrons leave the Si valence band before being trapped by a hydrogen atom, which acts as an electron sink. The pH of the solution controls oxidation/reduction rates. H-Si NWs surface slowly changes its character toward a more hydrophilic nature due to the appearance of partially protonated hydroxyl groups. When the dye is adsorbed on the active site, oxidative degradation takes place. The authors observed that degradation efficiency strictly depends on the crystal structure orientation of the NWs, as (100) Si substrates exhibited higher performance.

Table 5. NW-based catalyst used during photodegradation of various substrates. Copyright (2022) Elsevier.

Catalyst	Reduced substrate	Ref.
H-Si NWs	Methylene blue Methyl orange	150
ZnO NWs/Carbon fibers	Methylene blue	151
GaN NWs	Orange II	152
Cu_2Se NWs	Malachite green	153
$NaNbO_3/g\text{-}C_3N_4$	CO_2	154

Furthermore, ZnO NWs – carbon fiber composite prepared by Xue demonstrated enhanced photocatalytic properties thanks to ZnO piezoelectric nature [151]. Nanowire vertical alignment resulted in the formation of a 3D structure. Deformed ZnO NWs provided improved migration of charge carriers (electrons and holes). This study showed the synergistic effects of solar and mechanical energies in ecological industrial wastewater treatment. However, other key aspects of environmental samples could still damage such state-of-the-art nanocatalysts during their application. ZnO NWs are pH-sensitive, which strongly affects their catalytic properties under harsh conditions, which are common for industrial wastes.

Therefore, some interest was transferred to more resistant alternatives. Gallium nitride NWs exhibited outstanding stability under extreme pH values [152]. The highest performance in Orange II degradation was achieved at pH = 3.4, which is beneficial for real-life applications. As pH affects the space charge layer and redox potential, catalysts should be designed based on their resistance to more acidic regimes, rather than focusing only on overall catalytic activities. More examples of nanowires used in photocatalysis include Cu_2Se NWs for malachite green degradation, where a connection between NWs aspect ratio and reaction speed was observed [153]. Density functional theory (DFT) calculations unravelled the influence of specific atomic charge distribution on photocatalytic performance.

A slightly different application was found for $NaNbO_3$ NWs coupled with polymeric graphitic carbon nitride which were able to transform CO_2 into CH_4 using reduction [154] (Table 5). As described by Shi, photocatalysis may be also an interesting pathway for environmentally friendly and cheap fuels.

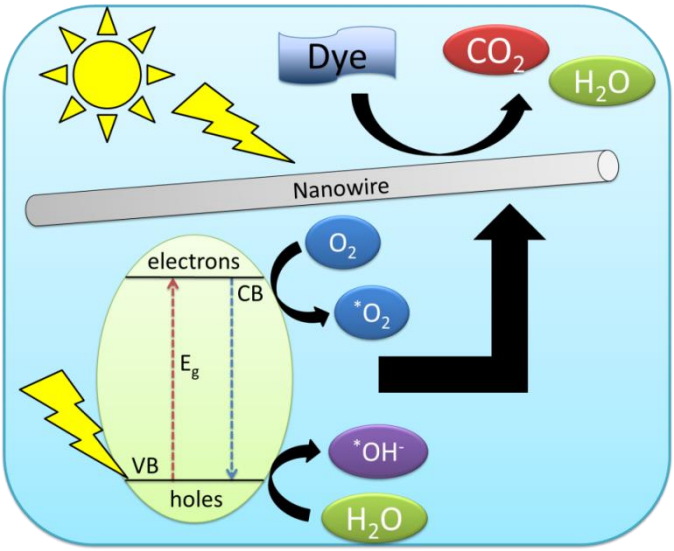

Fig. 7. Scheme of nanowire-driven photodegradation of dyes.

Presented catalytic applications, prove that nanowires are interesting alternatives for other bulk and nanostructured materials. They can be exploited as main catalysts, a support material, or an improver of catalytic properties, which makes them multipurpose, versatile, and easy-to-tune platforms. The main features of nanowires include their well-developed surface area, anisotropic morphology, and unique electronic properties. A wide spectrum of possible chemical compositions generates almost endless opportunities for nanomaterials in catalysis.

2. Aims and scope of the work

This thesis is focused on the synthesis of nanomaterials and their application as catalysts for organic chemistry reactions. Nanowires were chosen as primary nanoscale objects to study since they are not explored extensively enough in catalysis-related literature. Their composition was based on inexpensive and abundant elements such as copper, nickel, and cobalt. For improving performance of formed catalytic systems, a small amount of noble metal nanoparticles was implemented as highly active catalytic sites. The synthetic paths involved in this thesis comprised essential chemical transformations of great importance for chemical industry. The developed methods and techniques used were convenient and unsophisticated in practice which in the future could be easily scaled up. The following works described in this dissertation include:

- Synthesis of bimetallic nanowires from highly toxic industrial wastewater
- Decoration of metallic nanowires with nanoparticles to obtain composite nanocatalysts for coupling reaction to obtain small organic molecules and conjugated polymers
- Design and application of trimetallic nanocomposite as electrocatalyst for ethanol electrooxidation

Obtained nanomaterials were characterized by various techniques, which provided essential information and insight into possible assembly mechanism and their catalytic properties. The discussed results were published in reputed scientific journals, which underline the significance of the accomplished goals.

3. Results and discussion

3.1. Recycling of heavy metals by transforming industrial wastewater into Cu-Ni nanowire composites

During my internship at Aalto University in Finland, along with scientists from the Department of Chemical and Metallurgical Engineering, I studied the synthesis of non-noble metal nanowires from industrial wastewater [P2]. Such complex mixtures are a critical issue due to high toxicity and growing volumes, however, it is also a perfect source of metal ions, which can be extracted and converted into useful materials. New approaches for refining and recycling heavy metals are highly desired due to ecological and economical aspects. To further extent, alternative routes for nanomaterials synthesis are also interesting topics to explore. This research was an opportunity to test complex solution as a precursor of anisotropic nanostructures.

I obtained environmental samples from copper electrorefining, which contained mainly copper, nickel, arsenic, and antimony. It was a highly acidic solution due to the high concentration of sulphuric acid used during industrial processing, as revealed by analysis conducted using Inductively Coupled Plasma Optical Emission Spectrometry (ICP-OES). I used the Chang protocol for Cu NWs synthesis as starting parameters for the study using the above-mentioned source of metal ions [155]. I diluted the source material with deionized water to obtain a lower concentration of Cu and Ni ions, therefore gaining similar conditions as in the aforementioned paper. The synthesis required a highly alkaline medium, which was provided by a NaOH solution of 8-12 M, added to the diluted precursor. After heating the base solution to 60-85°C, I added ethylenediamine (EDA) as a capping agent to promote anisotropic growth and hydrazine (N_2H_4), as a reducing agent. This resulted in the precipitation of red flakes, which quickly turned black. Reactions were conducted for 10-60 min, and products were magnetically separated, washed with deionized water, and dried in air at 100°C. A schematic illustration of this process is covered in Figure 8.

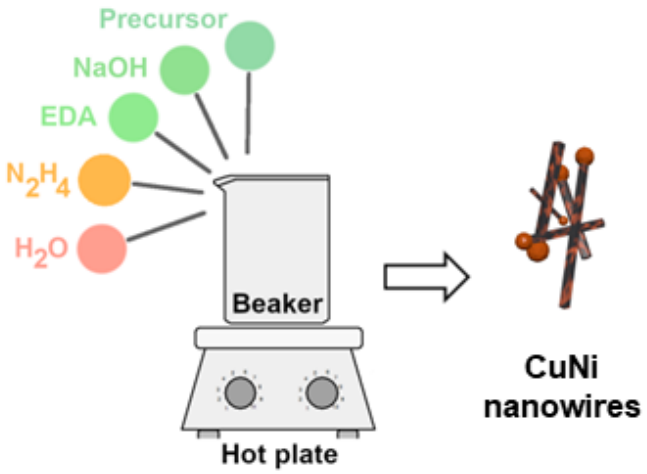

Fig. 8. Scheme of the synthesis procedure**.** Reproduced with permission from [156]. Copyright (2020) Springer Nature.

Co-precipitation of main components of the precursor solution can be described as follows:

$$2Cu^{2+} + N_2H_4 + 4OH^- \rightarrow 2Cu + N_2 + 4H_2O \quad \textbf{(6)}$$

$$2Ni^{2+} + N_2H_4 + 4OH^- \rightarrow 2Ni + N_2 + 4H_2O \quad \textbf{(7)}$$

A more detailed nanowire growth mechanism can be explained in a couple of steps. Cu^{2+} ions present in the basic environment form $Cu(OH)_4^{2-}$ complex molecules are reduced by hydrazine to $Cu(OH)_2^-$. Further reduction results in the formation of Cu_2O nano-seeds, which enable anisotropic growth on (110) plane [157,158]. Simultaneously, nickel hydroxide transforms into pure metallic atoms, which co-precipitate along the axis designated by the Cu_2O seed. During the growth, EDA controls the thickness of growing nanowires, by adsorption on sidewalls and thus blocking the building up of additional atoms. The whole process can be seen in Figure 9.

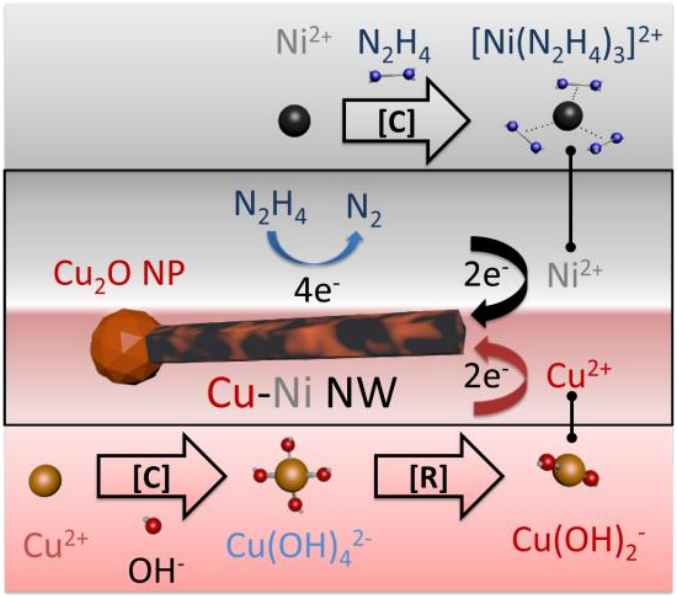

Fig. 9. Growth of a CuNi NW. [C] complexation, [R] reduction. Reproduced with permission from [156]. Copyright (2020) Springer Nature.

Once the first sample (S1) was obtained, its characterization by Scanning Electron Microscopy (SEM) revealed promising structures resembling nanowires, however, their irregularity and twisted nature distanced them from a true anisotropic nanostructure. I tried to optimize parameters such as temperature, concentrations of reaction components, and pH value, to improve homogeneity and purity of nanowires. Temperature studies showed that, at a certain point, at 80°C nanoparticles aggregate, which is a result of accelerated Cu_2O formation (S9, Fig. 10). This led to insufficient Cu^{2+} supply for proper growth of NWs. The main focus was dedicated to studying the importance of different reactant concentrations. The precursor solution was diluted to three levels, which were 0.03 M, 0.06 M, and 0.12 M of copper ions. The highest concentration gave mostly nanoparticles with a rough surface (S23, Fig. 10). In conclusion, anisotropic growth seemed to be limited in favor of the formation of more spherical nanostructures. Lower concentrations resulted in better morphologies, which proved the stated concept.

Hydrazine, as a reducing agent, had a significant impact on forming nanomaterials. When 0.2 mL of N_2H_4 was applied, the growth was uneven in all directions, and seed particles were preferred. Lesser values gave expected outcomes of NWs and nanorods based on literature knowledge [155,158]. However, their morphology was hindered by a

small coating of spherical nanoparticles. To tackle this inconvenience, the temperature was elevated to 70°C, which deleted unwanted elements from the nanomaterial. Unfortunately, for 0.2 mL N_2H_4, a similar test resulted in aggregated spherical nanoparticles. It can be concluded that radial growth was promoted, which increased the sizes of formed particles and therefore destroyed anisotropic morphology. Another reactant involved in NW synthesis was a capping agent. It was found that EDA concentration was crucial for desired nanostructure production. Higher concentration allowed for longer NWs growth (S13, Fig. 10). Encouraged by those findings, I tested EDA influence under elevated temperature, which led to thinner NWs and their moderate lengths.

Then, I extended the reaction time, which displayed, that after a standard 10 min reaction, plenty of metal ions remained unreacted. Additional time allowed for further growth of NWs, even up to 10 µm long (S15, Fig. 10). Visible spheres at the ends of NWs corresponded to Cu_2O seeds, which was also reported by Rathmell [158]. Lastly, I investigated the impact of the basicity of the reaction mixture. At starting temperature (60°C) 12 M NaOH solution gave thin NWs (S16, Fig. 10), however, increased temperature diversified morphologies of produced nanostructures (S17, Fig 10). I concluded that a higher concentration of OH^- accelerated complexes formation and thus a rapid nanoparticle seeding. As growth initiation was promoted over the propagation of anisotropic nanostructure, obtained nanomaterials were characterized in shorter lengths.

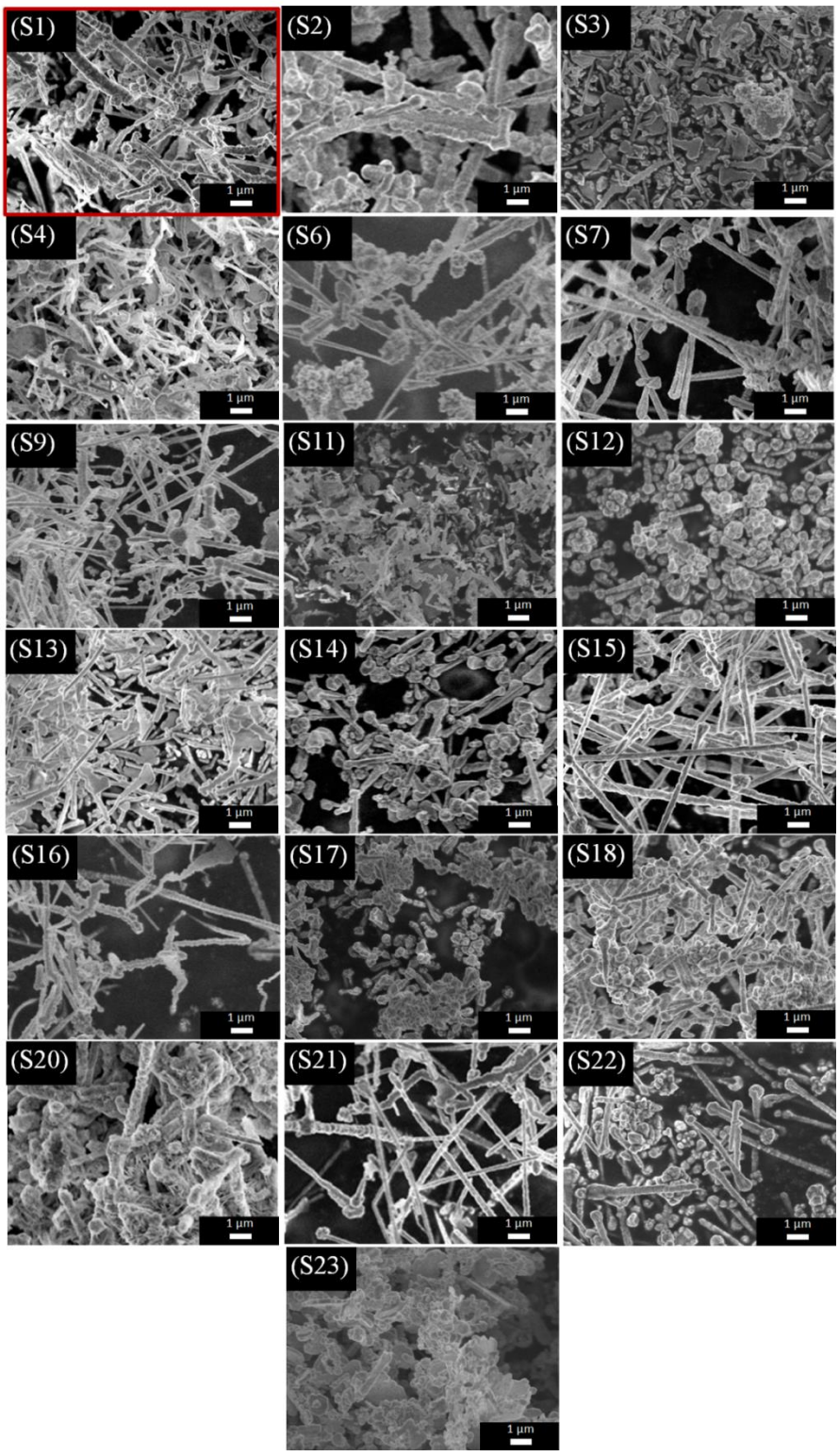

Fig. 10. SEM micrographs of the obtained selected nanostructures. SEM micrograph of the first sample produced using reference conditions is highlighted (denoted as S1 in the text). Reproduced with permission from [156]. Copyright (2020) Springer Nature.

After tuning reaction parameters, I concluded that S15 gave the best results among conducted experiments. I discovered key parameters, which should be adjusted for proper NW growth. Firstly, precursor solution concentration is crucial as an excess of metal ions leads to unwanted radial growth of spherical nanoparticles. Secondly, the length of NWs strictly depends on the reduction rate. Thirdly, the capping agent is the main factor in the anisotropic growth of NWs and must be dosed appropriately, so the full encapsulation of NWs may be omitted. Lastly, prolonged time is needed for higher conversion of starting material into advanced nanostructures. I also observed that under applied conditions only Cu and Ni were present, which was proved by Energy-dispersive X-ray spectroscopy (EDX) analysis (Figure 5a - P2). Visible elements were dispersed randomly along nanostructures, which excluded the possibility of formation of core-shell structure.

To summarize, I was able to achieve promising results by utilizing simple wet chemical reduction under controlled conditions to transform industrial wastes into nanostructures. The presented approach may attract more attention to 1D nanostructures due to the possible collaboration of industrial partners with nanostructures-focused research groups. As heavy metals-rich industrial wastewater is such a burning issue, an eco-friendly solution with additional benefits of nanowire synthesis seems to be a huge opportunity to exploit on a large scale. This topic is still an open field with spacious room for improvement and experimenting like various reducing and capping agents or different metals for alloying with copper. The obtained findings may become foundations for further studies targeting synthesis of nanowires from complex industrial wastes.

3.2. PdNPs/NiNWs as catalytic platform for Suzuki coupling of anisole derivatives

As discussed previously in this thesis, a coupling reaction is an efficient way of joining smaller molecules into larger and more complex chemical structures. Rapid development of catalytic platforms for such transformations is crucial due to their involvement in synthetic routes of fine chemicals, especially pharmaceuticals. Suzuki-Miyaura reaction is particularly essential, as the organoboron and organohalide substrate range contains numerous easy-to-handle species. Additional attention comes from important drugs, which are produced thanks to this reaction such as Losartan, Diflunisal, or Clonazepam [159]. Suzuki reaction is dominated by homogeneous complex-based palladium catalysts, which are expensive, and inconvenient, and their production yields toxic by-products [160–162]. Those issues hamper the large-scale application of coupling reactions. To overcome such limitations scientists are in search of an alternative approach to heterogeneous catalysis, particularly, by exploiting nanostructures. I joined those efforts by creating Pd decorated Ni NWs, which showed promising results in the catalysis of Suzuki cross-coupling [P3].

Metallic nanowires, which acted as magnetic support material, were prepared by simple wet chemical reduction of precursor solution with hydrazine. Self-assembly of Ni atoms was enhanced by applying an external magnetic field, which improved anisotropic growth by aligning metal atoms along the field. A more detailed analysis of NW synthesis can be found elsewhere [40]. The main advantages of this approach are rapid reaction and simplified product separation due to the ferromagnetic properties of nickel.

Palladium nanoparticles were deposited on NW surfaces by sonochemical technique, using K_2PdCl_4 as a palladium source and polyvinylpyrrolidone (PVP) as a capping agent for better control over growth. Additionally, PVP helped in the generation of free radicals, which were used to reduce Pd ions to metallic form. Those steps resulted in nickel anisotropic structures with spikes along their surfaces, coated by palladium spherical nanoparticles, which can be observed on Scanning Transmission Electron Microscopy (STEM) micrographs (Fig. 11).

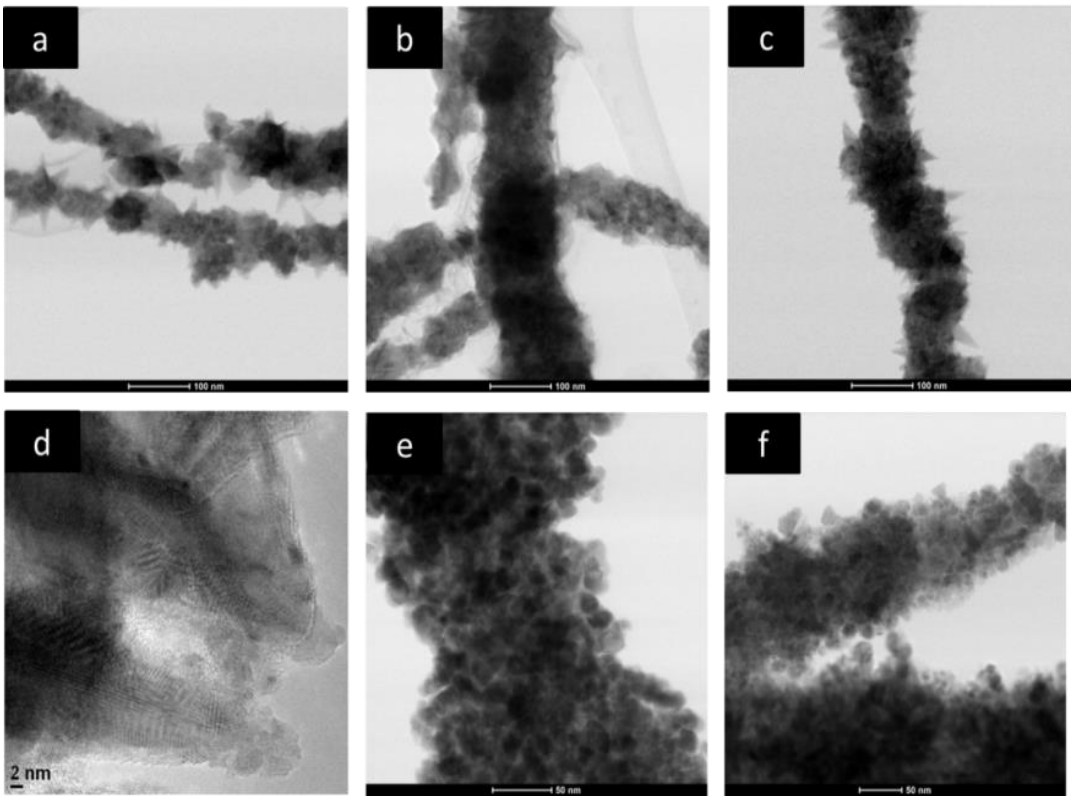

Fig. 11. STEM and TEM micrographs of PdNP/NiNW samples prepared with different Pd^{2+} concentrations: a,d– 5mM (S1); b,e – 10mM (S2); c,f – 15mM (S3). Reproduced with permission from [163]. Copyright (2023) Elsevier.

Selected area electron diffraction (SAED) patterning showed (111), (200), (220) faces for Ni and (111), and (220) faces for Pd (Fig. 12 a,b). X-ray photoelectron spectroscopy (XPS) allowed for a more precise analysis of chemical structure. Species like Ni_2O_3 (856.6 eV) and $Ni(OH)_2$ (855.4 eV), Pd (335.8 eV), and PdO (337 eV) were detected (Fig. 12 c).

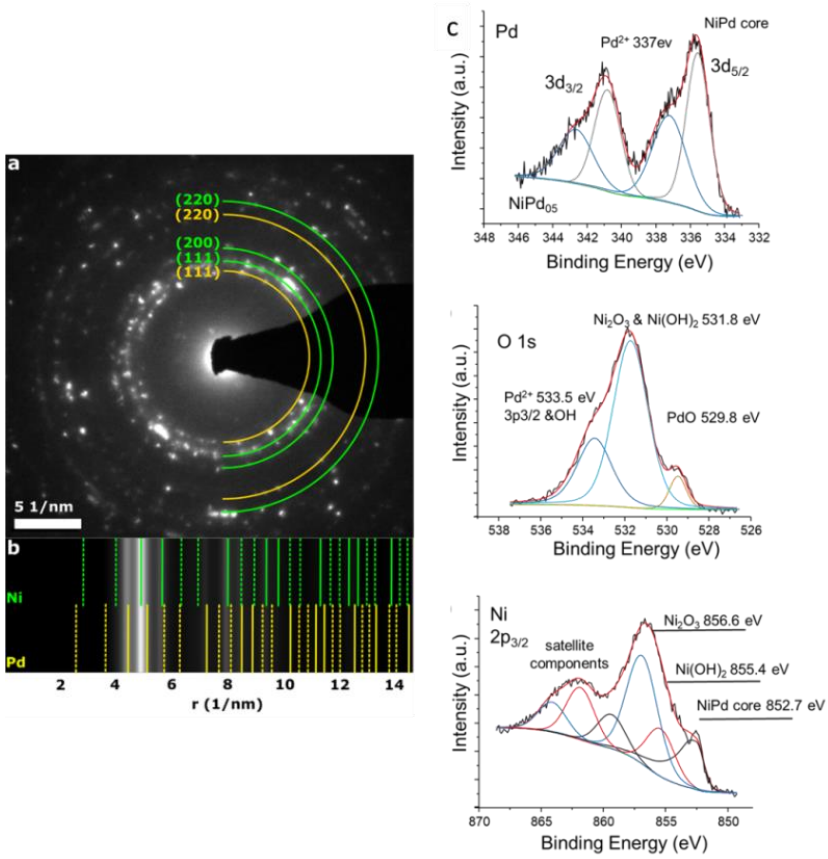

Fig. 12. (a) SAED pattern with marked Miller indices characteristic for metallic Pd and Ni together with (b) linear profiles confirming the coexistence of Ni and Pd phases in the analyzed sample S1. (c) X-ray photoemission spectra recorded for S1. Reproduced and modified with permission from [163]. Copyright (2023) Elsevier.

The catalytic study of as-prepared and characterized catalysts began with a model reaction of biphenyl synthesis from phenylboronic acid and bromobenzene (Reaction 8). Reaction conditions like solvent, temperature, and base were inspired by literature sources containing similar Pd catalysts [164–167]. First tests conducted in DMF: H_2O environment ensured aggregation leading to lower activity, especially for samples with higher concentrations of Pd. An extended reaction time of up to 24 h and elevated temperature (70°C) was needed to obtain quantitative yields. After tuning the parameters, S1 with the lowest Pd content exhibited improved results and even 100% yield (Table 7). Therefore, further studies were focused on that specific catalytic sample.

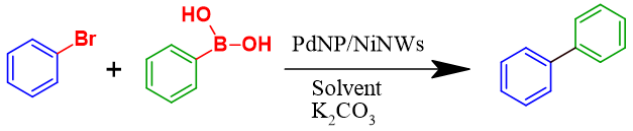

(8)

Table 7. Suzuki coupling of bromobenzene and phenylboronic acid on nanocatalysts with various Pd concentrations. Reproduced with permission from [163]. Copyright (2023) Elsevier.

%mass Pd	K_2CO_3 [mmol]	Temp [°C]	Time [h]	Solvent	Isolated Yield [%]	TOF [min^{-1}]
4.80%	1	60	3	DMF/H_2O	35%	0.21
2.00%	1	60	3	DMF/H_2O	50%	0.74
2.00%	2	60	3	DMF/H_2O	39%	0.57
2.00%	1	70	24	DMF/H_2O	89%	0.16
2.00%	2	70	24	DMF/H_2O	65%	0.12
0.34%	2	60	3	DMF/H_2O	47%	0.89
0.34%	1	60	3	DMF/H_2O	79%	1.00
0.34%	2	60	24	DMF/H_2O	51%	0.86
0.34%	1	60	24	DMF/H_2O	87%	0.92
0.34%	1	70	24	DMF/H_2O	100%	1.01

Reaction conditions: 0.75 mmol of phenylboronic acid, 0.5 mmol of bromobenzene, 2 mL DMF, 2 mL H_2O, 10 mg of nanocatalyst.

Unfortunately, after switching from bromobenzene to 4-bromoanisole (Reaction 9), yields decreased drastically. However, applying a different organic solvent (ethanol), enhanced the yield of the synthesis of 4-methoxybiphenyl to 79%. This resulted also in less toxic and easier post-treatment workup due to lower boiling point of ethanol. Iodo-derivatives performed as expected [168]. A steric hindrance limited the transformation of meta-substituted substrates in comparison to para- (85% vs. 93% yields). Positive outcomes were limited by low TOF values of 1.01 min^{-1}, which needed to be improved.

As conventional heating had some drawbacks such as temperature gradient in the reaction vessel, and undesirable catalyst agglomeration on the walls during vigorous stirring, a different approach had to be pursued. A microwave reactor was used for further study to solve the aforementioned issues. It allowed a time reduction from 24 hours to only 15 minutes, which improved TOF values significantly. The parameter study resulted in enhanced yields for anisole and toluene derivatives above 80% and 70% respectively (Table 8). Other moieties such as nitro-, hydroxyl- esters, and carbonyl- were also tested, however, without any success. Therefore, it can be

concluded that prepared PdNPs/NiNWs composite catalyst exhibits high selectivity towards anisoles and toluenes.

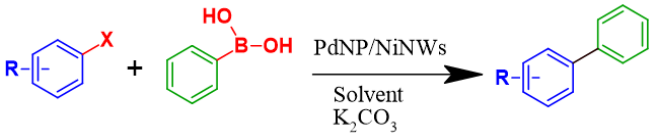

(9)

Table 8. Suzuki coupling of various halo-derivatives with phenylboronic acid in the presence of microwaves (Reaction 9). Reproduced and modified with permission from [163]. Copyright (2023) Elsevier.

R	X	K_2CO_3 [mmol]	Temp. [°C]	Time [min]	Isolated Yield [%]	TOF [min^{-1}]
4-OMe	Br	2	70	15	48%	49.88
4-OMe	Br	1	70	15	77%	80.02
4-OMe	Br	1	90	15	95%	98.73
4-OMe	Br	1	110	15	87%	90.41
3-OMe	Br	2	70	15	96%	99.76
3-OMe	Br	1	70	15	76%	78.98
3-OMe	Br	2	90	15	100%	103.92
3-OMe	Br	2	110	15	85%	88.33
4-Me	Br	2	70	15	27%	28.06
4-Me	Br	1	70	15	18%	18.71
4-Me	Br	2	90	15	40%	41.57
4-Me	Br	2	110	15	70%	72.75
4-MeO	Br	2	70	15	0%	0.00
4-OH	Br	2	70	15	0%	0.00
4-NO_2	Br	2	70	15	0%	0.00
4-OMe	I	2	70	15	97%	100.80
4-OMe	I	1	70	15	36%	37.41
4-OMe	I	2	90	15	79%	82.10
4-OMe	I	2	110	15	85%	88.33
4-COOMe	I	2	70	15	0%	0.00

Reaction conditions: 0.75 mmol of phenylboronic acid, 0.5 mmol of aryl halide, 2 mL EtOH, 2 mL H_2O, 10 mg of nanocatalyst (0.34% Pd/NiNWs).

To boost the TOF value even higher, the reaction time was shortened to 10 and 5 min, which showed only a small variation in yields (Table 9). The catalyst load was also lowered from 10 mg down to 2 mg for 15 min reaction, which resulted in an astonishing 519.61 min^{-1} TOF.

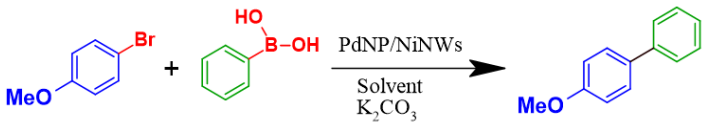

(10)

Table 9. Reduction of reaction time and catalyst load for coupling of 4-bromoanisole with phenylboronic acid (Reaction 10). Reproduced and modified with permission from [163]. Copyright (2023) Elsevier.

Catalyst load [mg]	K_2CO_3 [mmol]	Temp. [°C]	Time [min]	Solvent	Isolated Yield [%]	TOF [min^{-1}]
10	1	90	15	EtOH/H_2O	95%	98.73
10	1	90	10	EtOH/H_2O	97%	151.21
10	1	90	5	EtOH/H_2O	95%	296.18
5	1	90	15	EtOH/H_2O	100%	207.84
2	1	90	15	EtOH/H_2O	100%	519.61

Reaction conditions: 0.75 mmol of phenylboronic acid, 0.5 mmol of aryl halide, 2 mL organic solvent, 2 mL H_2O.

The stability of the new catalytic system was also investigated. 4-bromoanisole was chosen as substrate and the reaction was conducted 5x, subsequently washing/drying of the same portion of the catalyst. The three first cycles showed a minor decrease in 4-methoxybiphenyl yield (93%→87%→84%), however, the fourth cycle gave a higher yield than starting reaction (99%), which again decreased in 5th cycle to 95%. Such a phenomenon may be connected to the activation of the catalyst during consequential reactions.

I concluded that microwave irradiation plays a vital role in the catalytic cycle of studied composite nanomaterial. A more direct approach to heating the molecules was beneficial due to the removal of the temperature gradient inside the reaction mixture. This resulted in faster reaction times, as kinetics were enhanced significantly. The metallic character of the prepared catalyst caused the occurrence of high voltage current due to electron oscillation [169]. Sparking and plasma discharging created hot spots due to the Joule heating phenomenon (Fig. 13). As a result, improved diffusion, heat, and mass transfers occurred. Conducted experiments showed huge differences in reaction rates and yields of conventional and microwave approaches, which confirmed the hypothesis.

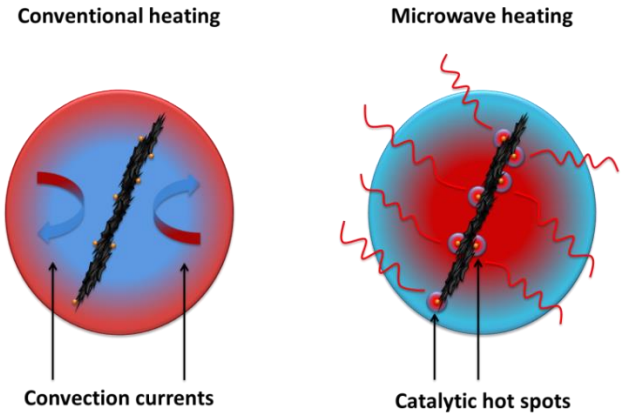

Fig. 13. Comparison of conventional and microwave heating approaches of the reaction mixture. Reproduced with permission from [163]. Copyright (2023) Elsevier.

The reaction mechanism followed a classical palladium-driven Suzuki coupling catalytic cycle. Due to an alternative heating method, I speculated that the first step was the generation of hot spots on PdNPs due to microwave irradiation. As-created active species released Pd atoms by leaching into the reaction medium, which acted similarly to a typical Suzuki catalyst (Fig. 14). Textbook subsequent stages of oxidative addition, transmetalation, and reductive elimination occurred conventionally. Then Pd^0 atoms redeposited on NWs, however, in different places due to entropy. This may explain the observed behavior of recycled catalysts, in which the redistribution of Pd atoms self-tuned overall properties.

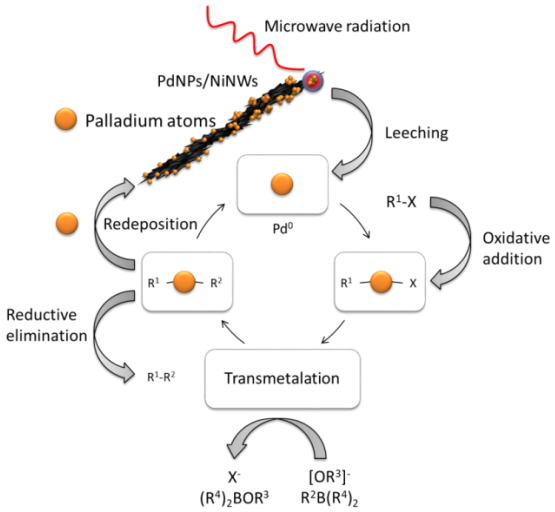

Fig. 14. Proposed mechanism for the PdNPs/NiNWs-catalyzed Suzuki cross-coupling reaction. Reproduced with permission from [163]. Copyright (2023) Elsevier.

In summary, a new catalytic system was created, characterized, and exploited in the coupling reaction. Palladium-decorated nickel nanowires were obtained by an inexpensive and convenient synthesis protocol, which offers scale-up opportunities. A specific selectivity towards anisole and toluene derivatives was observed during catalytic reactions. Despite moderate to quantitative yields under conventional heating, studies involved microwave irradiation, which boosted the catalytic properties of PdNPs/NiNWs to a further extent. A vast time reduction enabled by this approach allowed taking it down from one day to an outstanding 5 minutes. Simplified separation of catalyst from post-reaction medium, due to magnetic properties, was another beneficial outcome of PdNPs/NiNWs-driven reactions. This study showed how important nanomaterials are during the development of modern catalysts for advanced chemical transformations. Their notable catalytic activities, promoted by well-developed surface area and quantum effects can be further enhanced by synergistic effects, by alloying and composing them together into highly efficient catalytic platforms.

3.3. Nanocatalytic approach for polyfluorene derivative synthesis by applying microwave radiation to PdNPs/NiNWs catalyst

This work [P4] is an expansion of the previously presented concept of the Suzuki coupling reaction, whose promising results encouraged further research on larger chemical species. π-conjugated polymers are substances with a bountiful variety of chemical structures. They proved to be versatile tools for photovoltaics [170,171], organic light-emitting diodes (OLEDs) [172,173], and other electronic devices [174,175]. They also possess other interesting properties such as the ability to extract specific chiralities of carbon nanotubes. Structure-dependent selectivity corresponds to π-π and CH-π interactions during polymer adsorption onto CNT walls. This characteristic behavior, being exploited by numerous research teams [176–179], made conjugated polymers valuable materials. Conjugated polymer extraction (CPE) emerged as a promising solution compared to other single-walled carbon nanotube (SWCNT) purification methods such as electrophoresis [180], density gradient centrifugation [181], or chromatography [182]. However, their synthesis struggles with optimization and mass

control. Inhomogeneous polymers, which differ from batch to batch hinder SWCNTs separation [183]. Therefore, crucial efforts have to be made to improve their synthesis protocols. The most common synthetic route involves the Suzuki polycondensation reaction, which can be A-B or AA-BB types, according to used diaryl bromides and diaryl boronate esters. It is catalyzed by palladium complexes such as tetrakis(triphenylphosphine) palladium (0) - $(Pd(PPh_3)_4$. Although it possesses high activity and selectivity, a set of drawbacks hinder industrial application. Due to phosphine ligands, the production process is expensive and yields toxic by-products. Furthermore, an oxygen-free reaction atmosphere is needed to ensure complex stability. As a homogeneous catalyst, recyclability is almost impossible. Those issues declassify complexes in terms of profitable catalysts for cheap polymerization protocols.

To compensate for the listed problems, I applied PdNPs/NiNWs as a nanotechnological approach in Suzuki polycondensation (Fig. 15). The catalyst was prepared similarly to the one in previously presented article. It is worth mentioning that during publishing this was the first attempt at using such a catalytic system in this kind of reaction. In addition to catalysis studies, obtained polymers were exploited in CPE protocols, in which an enriched (7,5) SWCNT chirality fraction was successfully extracted from polychiral raw material.

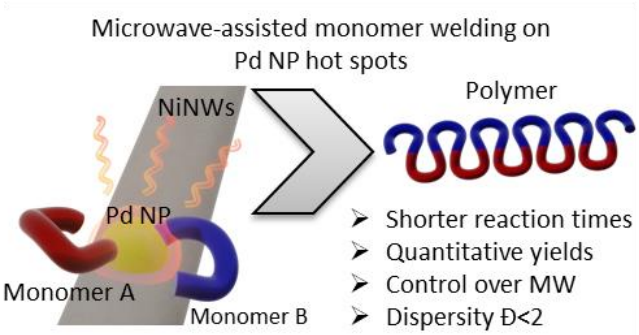

Fig. 15. Illustrative expression of key aspects of [P4]. Reproduced with permission from [184]. Copyright (2024) Springer Nature.

For investigation of catalytic properties, a fluorene-based polymer was chosen as the targeted product, precisely poly (9,9-dioctylfluorenyl-2,7-diyl) (PFO) (Reaction 11). After preparation of 0.34%PdNPs/NiNWs catalyst, the initial experiment was

performed in the same manner as for $Pd(PPh_3)_4$-promoted synthesis. This included a sealed reactor containing reactants and solvents. Magnetic stirring and conventional heating were applied for three days, after which the commercial catalyst gave 83% polymer yield, and the nanocatalyst performed poorly by reaching only 16% dimers yield. I suspected that the paramagnetic properties of NWs resulted in strong aggregation around Teflon-coated dipole. It might have caused a major decrease in the catalytic activity of the tested sample. As microwave irradiation proved to enhance catalytic properties in previous research and many other literature examples [185,186], further studies involved microwave reactors. Once again, the alternative heating method proved to be more efficient, compared to the conventional approach. However, during this research, a more detailed investigation of energy supply was conducted, by applying two different modes. A Standard Mode (SM) reached the designated temperature by varying microwave power. After that temperature oscillated around the target value with a 1°C buffer. The second mode called Solid Phase Synthesis (SPS) relied on constant power. The target temperature range was achieved under a stable supply of microwaves. A list of conducted experiments may be found below (Table 10).

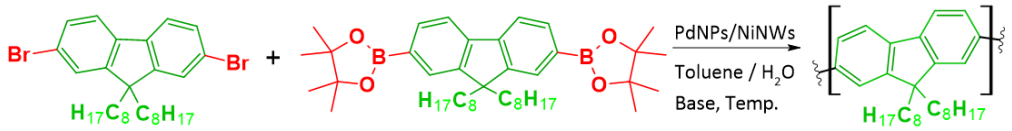

(11)

Table 10. Microwave-assisted PFO synthesis via Suzuki polycondensation at Standard and SPS modes. Reproduced and modified with permission from [184]. Copyright (2024) Springer Nature.

No.	Mode	Power [W]	Base/Conc.	T [°C]	Yield [%]	TOF [h^{-1}]	M_n [kg/mol]	M_w [kg/mol]	*Đ*
1	SM	0-200	Na_2CO_3/1M	80	0	-	-	-	-
2	SM	0-200	Na_2CO_3/1M	110	62	1793	1.88	3.06	1.63
3	SM	0-200	Na_2CO_3/1M	130	57	1648	8.08	11.31	1.40
4	SM	0-200	K_2CO_3/1M	80	34	983	3.14	3.99	1.27
5	SM	0-200	K_2CO_3/1M	110	69	1995	5.25	8.45	1.61
6	SM	0-200	K_2CO_3/1M	130	75	2168	4.56	6.61	1.45
7	SPS	80	Na_2CO_3/1M	75-80	0	-	-	-	-
8	SPS	80	Na_2CO_3/1M	105-110	82	2371	8.32	16.31	1.96
9	SPS	80	Na_2CO_3/1M	125-130	41	1185	4.95	6.68	1.35
10	SPS	80	K_2CO_3/1M	75-80	51	1475	3.45	4.59	1.33
11	SPS	80	K_2CO_3/1M	105-110	69	1995	6.61	11.90	1.80
12	SPS	80	K_2CO_3/1M	125-130	60	1735	6.19	8.66	1.40
13	SPS	100	Na_2CO_3/1M	105-110	88	2544	14.32	25.99	1.82
14	SPS	120	Na_2CO_3/1M	105-110	78	2255	8.37	12.67	1.51

Reaction conditions: 0.12 mmol of diarylbromide, 0.12 mmol of diarylboronate ester, 2 mL of base solution, 2 mL of toluene, 1 drop of Alliquat 336, and 10 mg of PdNPs/NiNWs catalyst. The reaction was carried out for 1 hour. The degree of polymerization was estimated by dividing M_n by monomer mass (0.388 kg/mol).

In both microwave modes, reaction times were shortened from 3 days of conventional heating down to 1 hour. In most conducted experiments, polymer yields exceeded 60%, which was a significant improvement compared to the previously presented yields. By tuning certain conditions such as temperature, heating mode, or base, a strong connection to molecular weight and yield was observed. Starting with thermal adjustment and sodium salt, the reaction under 80°C gave no polymer at all. This was reported for both microwave modes, which concluded that a higher temperature was needed for a reaction to occur at a satisfying rate. Therefore, it was increased to 110°C, which yielded oligomers (M_n=1.88 kg/mol) for Standard Mode and longer chains (M_n=8.32 kg/mol) for SPS mode. It is worth noting that in most cases, I observed a decrease in molecular weight when temperature was increased to 130°C. At this temperature, only sodium salt under the Standard program positively affected chain length and such reaction conditions resulted in a higher M_n of 8.08 kg/mol (compared to 1.88 kg/mol).

This showed how important the base is during Suzuki polycondensation. In literature, strong and weak bases are preferred according to used substrates and their reactivity [187–189]. As they allow quaternization of organoboron structures, and therefore increase their nucleophilicity. Consequently, it results in higher reactivity and accelerated polymerization process [190]. Due to the high impact on kinetic aspects of polycondensation, base choice can drastically alternate reaction outcomes. Microwave mode determined how much power was provided to the reaction vessel. A predicted behavior of Standard Mode could be expressed as a downhill function, where at the start the output power is high and slowly decreases over time to fairly consistent values of around 5-15 W at desired temperature. This provided a higher reaction rate in the first minutes of the experiment and after that lower power limited the maximum polymer chain length, which could grow in the designated time. Opposite conditions were applied by SPS mode, which released microwave power in short bursts to maintain reaction temperature in a specified regime. This mode delivered power to catalyst and reactants in more controlled and stable way leading to enhanced chain growth, which at certain conditions gave higher molecular weights (entry 8 - 8.32 kg/mol vs. entry 2 - 1.88 kg/mol and entry 11 - 6.61 kg/mol vs. entry 5 - 5.25 kg/mol in Table 10). This encouraged further testing of the influence of SPS power output. By applying 100 W I was able to obtain a polymer with M_w = 25.99 kg/mol, which corresponded roughly to 37 units of fluorene-derivative monomer. However, a further increase to 120 W resulted in shorter chains up to 22 units (M_w = 12.67 kg/mol).

The generation of hot spots on metallic nanostructures, provided by microwave heating, strongly affected process thermodynamics [191–193]. This phenomenon was amplified by SPS mode, where high power was delivered through whole synthesis, compared to Standard mode. Enhanced reactant diffusion and uniform heating of reaction volume improved the reaction rate and allowed the formation of longer chains. Palladium nanoparticles transformed into welding spots of high energy were a key aspect of accelerated polycondensation (Fig. 16). Furthermore, the homogeneity of the obtained polymers was satisfying. Dispersity indices (*Đ*) ranged between 1.27 and 1.96.

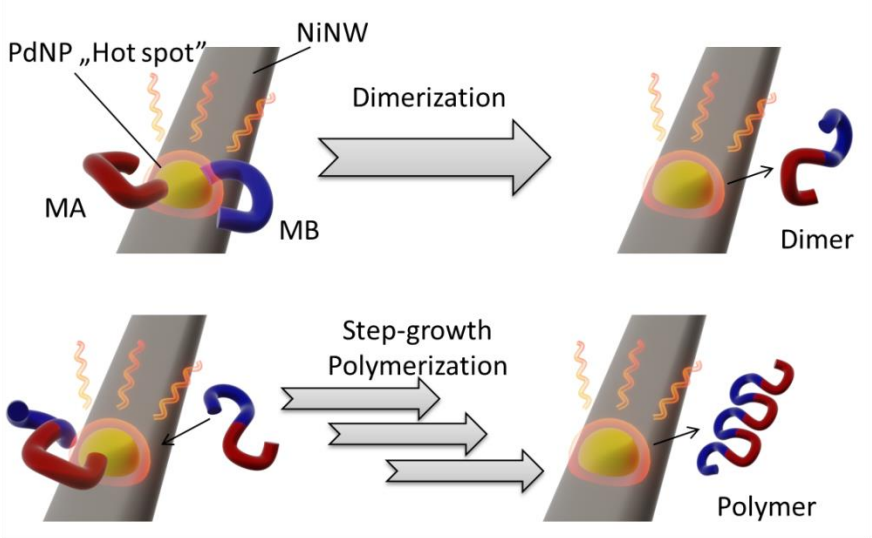

Fig. 16. Proposed mechanism of "hot spot" mediated step-growth Suzuki polymerization. MA and MB stand for Monomer A (diarylbromide) and Monomer B (diarylboronate ester), respectively. Reproduced with permission from [184]. Copyright (2024) Springer Nature.

To exhibit the potential applicability of obtained polymers, CPE protocols were used for the chirality-dependent separation of SWCNTs. A remarkable selectivity of PFO towards (7,5) chirality was presented previously [179,194]. Figure 17 shows UV-VIS spectra and Photoluminescence (PL) maps of prepared samples. Firstly, whole nanocarbon material was suspended with poly(9,9-dioctylfluorenyl-2,7-diyl-alt-3-dodecylthiophene-2,5-diyl) (PFO-3DDT) in toluene to reveal the composition of the raw material. UV-VIS spectra of this dispersion can be seen in Figure 17a, confirming the presence of a wide spectrum of SWCNT species. In the second experiment, synthesized PFO with higher molecular weights were used to achieve extraordinary (7,5)-enrichment, while PFO with shorter chains were more selective towards (6,5) SWCNTs as illustrated in the enclosed optical absorption spectra in Figure 17c. In PL maps (Fig 17b, d), numerous features can be observed for unselective PFO-3DDT dispersion, whereas PFO dispersion (Table 11 entry 13) exhibited a single peak coming from (7,5) SWCNT chirality.

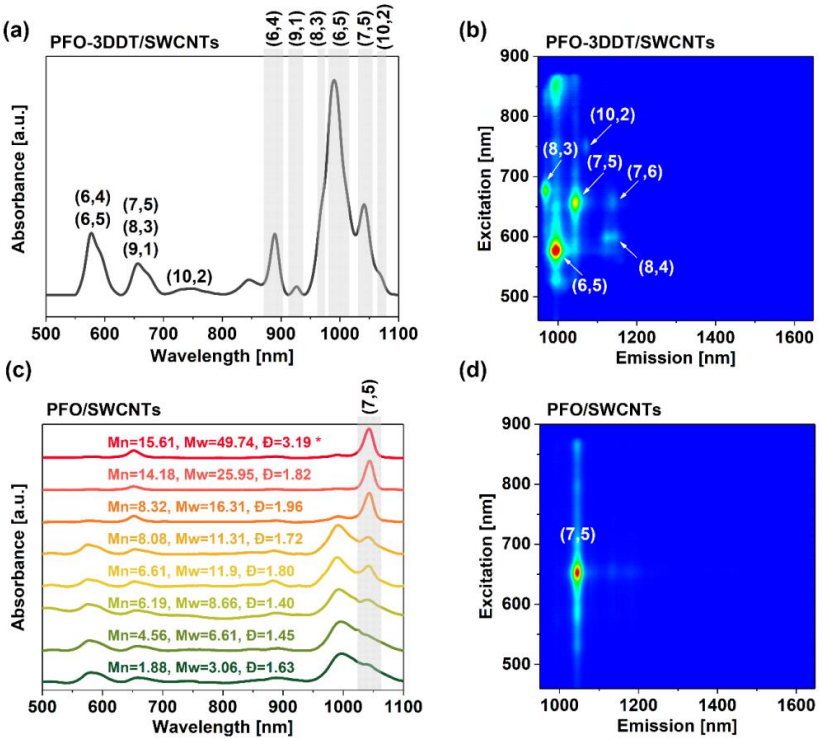

Fig. 17. (a) UV-VIS spectrum of SWCNTs suspended by PFO-3DDT**.** (b) Excitation-emission PL map of suspended material. (c) The influence of molecular characteristics of the synthesized PFO batches on the optical absorbance spectra of SWCNTs suspended with this polymer. Polymer with the highest molecular weight (49.74 kg/mol) refers to $Pd(PPh_3)_4$–driven reaction which is shown here as a reference, all the other polymers were obtained using PdNPs/NiNWs nanocatalyst. (b) excitation-emission PL map of extracted (7,5) SWCNTs using Table 1 - entry 13 polymer. Reproduced with permission from [184]. Copyright (2024) Springer Nature.

This study showed how the development of a new catalytic system can improve conjugated polymer synthesis. Quantitative yields proved the high activity of the presented catalyst. A wide range of molecular weights suggests possible tuning and optimization opportunities, which can lead to even more controlled polycondensation. Significant acceleration accomplished by applying microwave irradiation was another key advantage, which allowed a 1-hour reaction instead of 3 days of conventional heating. High quality of obtained polymer chains was characterized by low dispersity indices, which in all cases were below two. Additional utility factor in the form of (6,5) chirality isolation by produced polymers is also worth mentioning. Overall results show

an opportunity window for controlled and more convenient ways of conjugated polymer production.

3.4. Pd/Co-NiNWs as catalytic solution for direct ethanol fuel cells

The last work [P5] of this monothematic cycle is connected to electrocatalysis. Green and sustainable sources of electric power are a common focus of numerous studies, due to the never-ending electricity demand driven by the continuous development and growth of the human population. Alternatively, by considering sun, wind, and water [195,196], energy can be produced by chemical reactions. Direct extraction of electrical energy from stored sources can be achieved in fuel cells. Recently, this topic has become a crucial issue due to ecological regulations regarding fossil fuel exploitation. Alcohol electrooxidation is considered an alternative source of electricity for small devices and in the automobile industry. However, the electrochemical processes of chemical compound conversion, which yield electricity, require an efficient and stable catalytic system. Commonly used Pt-based systems are highly active and can work under mild conditions. Unfortunately, a list of drawbacks such as high vulnerability to CO poisoning, low abundance, and high market price, limits commercial application [197,198]. Therefore, more advanced catalysts are studied in this regard. I participated in such research, where I synthesized composite nanocatalyst for electrooxidation consisting of cobalt-nickel nanowires and palladium nanoparticles.

Nanostructures were prepared by a two-step protocol. During the first part, the cobalt-nickel nanowires of various molar ratios were obtained by the reduction of metal ions by hydrazine under a magnetic field, which enhanced anisotropic growth. Next, in a similar manner to previously discussed works, Pd nanoparticles were deposited by the sonochemical process. A set of nanocomposites exhibited different morphologies, according to designed chemical compositions. STEM images showed that a higher concentration of Co nanowires created a bead-like anisotropic structure, whereas the increase of Ni content created spikes along the surface. Those features had a key influence on nanowire surfaces and therefore, controlled palladium nanoparticle deposition. An X-ray diffraction (XRD) analysis showed a significant relation between

nanowire metal ratio and nanostructure. For Ni-rich samples, the cubic Ni(Co) phase was dominant. A highly disordered hexagonal $Co_{0.75}$-$Ni_{0.25}$ phase could be observed for the opposite situation regarding the concentration of both metals (Fig. 18). Moreover, STEM micrographs revealed plate-like structures surrounding NWs (Fig. 19). According to EDX analysis, such plates were composed of metallic oxides. Palladium was detected at the edges of those oxide layers.

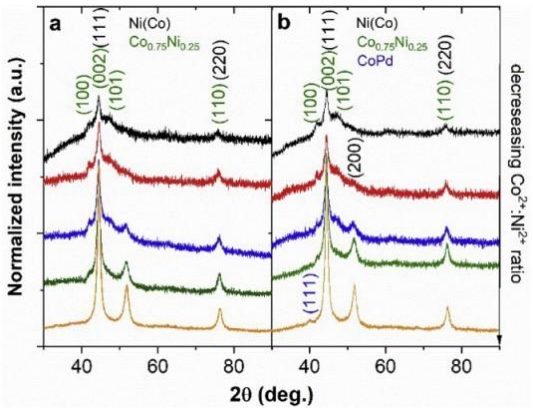

Fig. 18. XRD patterns of CoNi NWs synthesized using different Co:Ni ratios with marked peaks corresponding to the Ni(Co), $Co_{0.75}Ni_{25}$ phases and CoPd. Samples synthesized using 0.5 mM (a) and 0.75 mM (b) of K_2PdCl_4. (Co_9–Ni_1 - black curve, Co_7–Ni_3 - red curve, Co_5–Ni_5 - blue curve, Co_3–Ni_7 - green curve, Co_1–Ni_9 - orange curve). Reproduced with permission from [199]. Copyright (2022) Elsevier.

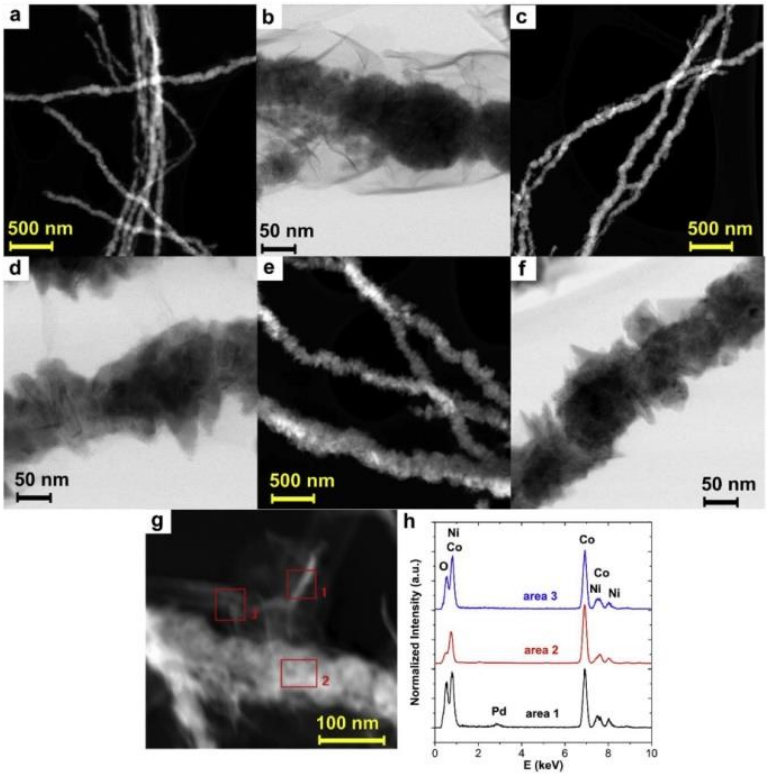

Fig. 19. STEM HAADF (a, c, e) and BF-DF (b, d, f) images of CoNi NWs synthesized using different Co:Ni precursor ratios: 9:1 (a, b), 5:5 (c, d) and 3:7 (e, f); (g) HAADF STEM image of CoNi NW synthesized using Co:Ni precursor ratio equal to 9:1 with marked areas and corresponding to them EDX spectra (h) confirming existence of Co and Ni oxides and Pd nanoparticles deposited on this oxidized surface. Reproduced with permission from [199]. Copyright (2022) Elsevier.

In high-resolution TEM (HRTEM) images of analysed samples, PdNPs were observed in two distinctive zones. The first one corresponded to the highly disordered core $Co_{0.75}Ni_{0.25}$ phase (Fig. 20a,b), whereas the second could be described as an oxidized plate-like surface of PdO_2NPs (Fig. 20c,d). Crystallization of palladium species occurred particularly on oxidized surfaces, however, few clusters were spotted on the crystalline Ni(Co) phase (Fig. 20d-f), and metallic PdNPs were observed on surfaces of Co_5-Ni_5NWs (Fig 20g,h). In conclusion, palladium ions crystalize as metallic particles and oxidized species, however, oxide nucleation occurs only on oxidized surfaces.

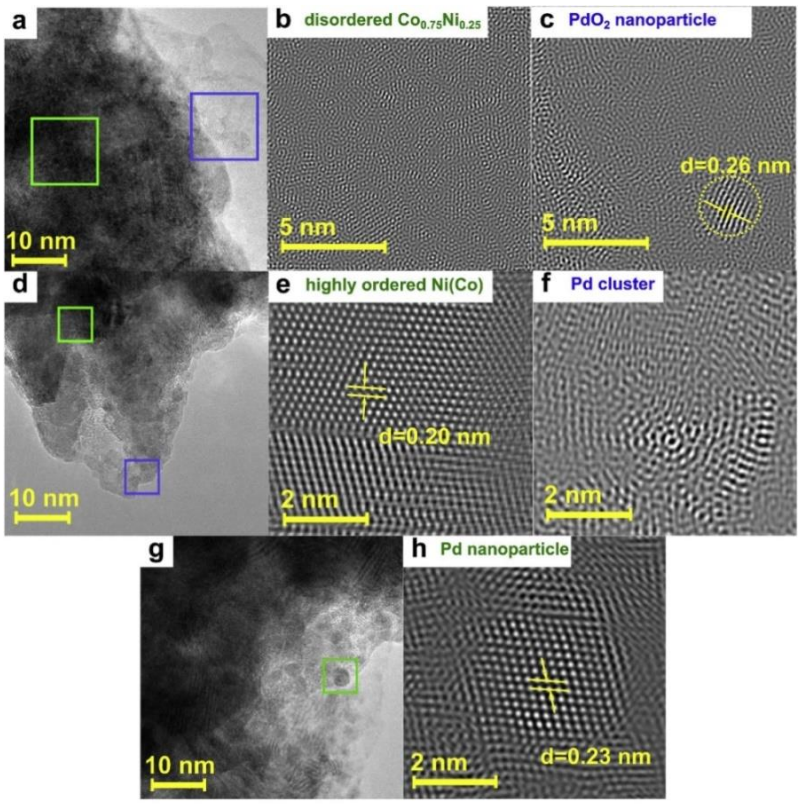

Fig. 20. HRTEM micrographs of CoNi NWs synthesized using Co:Ni precursors ratio: 9:1 (a-c), 3:7 (d-f) and 5:5 (g and h); (b) enlarged green marked area on (a) confirming existence of highly disordered $Co_{0.75}Ni_{0.25}$ hexagonal structure; (c) enlarged blue-marked area on (a) with identified interplanar distance characteristic for PdO_2 (101) planes; (e) enlarged green-marked area on (d) with identified interplanar distance characteristic for Ni (111) planes; (f) enlarged marked blue area on (d) confirming the existence of Pd atomic clusters at the edges of highly crystalline Ni phase; (h) enlarged green marked area on (g) with identified interplanar distance characteristic for Pd (111) planes. Reproduced with permission from [199]. Copyright (2022) Elsevier.

XPS analysis gave interesting results, which unraveled more information about Pd deposition (Fig. 21). Tests were performed on obtained nanocomposites and after Ar^+ treatment, which removed the oxidized layer. In contrast to Ni and Co, the palladium atomic concentration decreased with the depths of nanomaterial. Ni2p photoemission spectra exhibited Ni_2O_3, NiO, and Ni atoms building NW core at 856.6 eV, 854.4 eV, and 852.8 eV respectively [197,200]. Two components of $Co2p_{1/2}$ spectra were deconvoluted as Co_3O_4 (797.6 eV) and satellite structure. Pd 3d confirmed the presence of previously detected Pd and PdO_2 nanoparticles. A higher concentration of

Pd precursor resulted in lower PdO_2 peak intensity (Fig. 21g,h). This related to the preferable crystallization of metallic Pd form when the content of Pd^{2+} was sufficient. Removing of oxide layer revealed metallic nickel and cobalt along with minimal cobalt oxide inclusions.

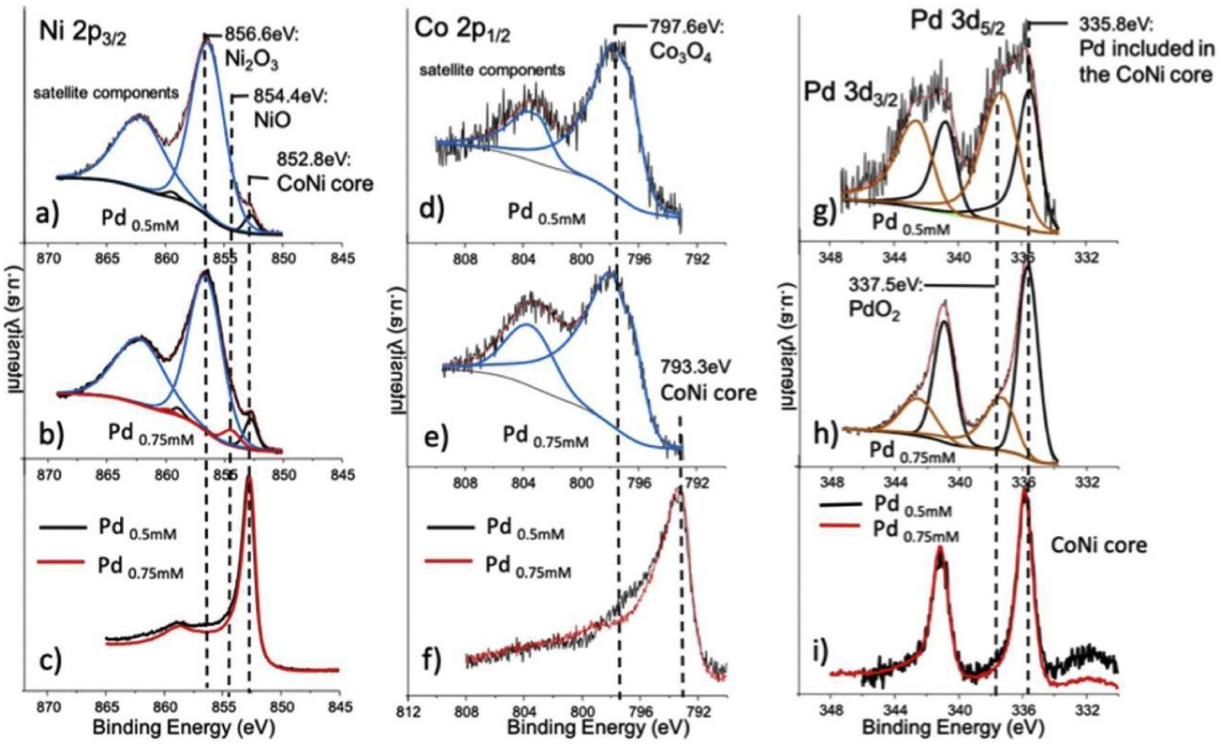

Fig. 21. $Ni2p_{3/2}$ (a, b and c), $Co2p_{1/2}$ (d, e and f) and $Pd3d_{5/2}$ (g, h and i) photoemission spectra recorded for CoNi NWs (Co:Ni ratio equal to 3:7) after deposition of Pd NPs using 0.5 mM of K_2PdCl_4 (a, d, g) and 0.75 mM of K_2PdCl_4 (b, e, h); the spectra on (c, f and i) were obtained after Ar^+ ion treatment procedure. Reproduced with permission from [199]. Copyright (2022) Elsevier.

After the characterization of nanomaterial, an electrocatalytic activity of the as-prepared composite was investigated by means of cyclic voltammetry (CV). First tests were run in 1 M NaOH and results of the fifth cycle were gathered in Figure 22. Peaks above 0.3 V corresponded to Pd oxidation and reduction of generated oxides, which was described in the literature [201].

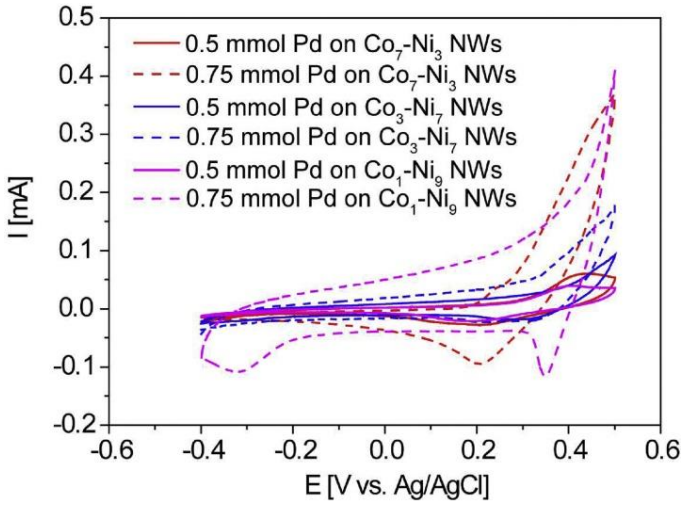

Fig. 22. Cyclic voltammetry curves of Co:Ni NWs decorated by Pd NPs in argon-saturated 1.0 M NaOH solution at a scan rate of 20 mV/s at room temperature. The solid lines present the results for electrocatalysts synthesized by using 0.5 mM palladium precursor, while the dashed lines by using 0.75 mM palladium precursor. Reproduced with permission from [199]. Copyright (2022) Elsevier.

To investigate catalytic activity towards application in fuel cells, ethanol electrooxidation was focused as a research subject, due to low toxicity and inexpensive sources of such fuel. The addition of ethanol into the electrolyte solution was followed by Ar bubbling in order to remove dissolved oxygen. The lowest catalytic activity was recorded for Co_5-Ni_5 and Co_9-Ni_1 samples. Passivated by plate-like oxides, the nanowire core was separated from PdO_2 deposited on the edges of those structures, which hindered the synergistic effect of the catalytic platform. Samples with higher Ni content exhibited less concentration of such obstacles. At metal ratio Co:Ni 1:9, Pd crystalized in metallic form, and thus catalytic activity was boosted significantly up to 2500 mA/mg_{Pd} for 1.92% Pd concentration. Nevertheless, optimization required a balanced phase nanostructure. On the other hand, Co_3-Ni_7 samples gave the highest mass activities due to the appropriate contribution of Ni(Co) cubic and highly disordered $Co_{0.75}Ni_{0.25}$ phases (5252 mA/mg_{Pd} for 0.5 mM Pd precursor and 8003 mA/mg_{Pd} for 0.75 mM) (Fig. 23a). The oxophilic nature of used metals facilitated the generation of OH_{ads} at lower potentials, which resulted in oxidative desorption of the intermediate products [202,203]. Also, the interface between Co-Ni NWs and Pd NPs induced charge transfer. High dispersion of active sites in the form of Pd nanoparticles,

well-developed surface area, and synergistic effects were the main reasons for enhanced catalytic performance. Furthermore, the interface between Co-Ni NWs and Pd NPs induced charge transfer, which strongly affected the overall catalytic activity.

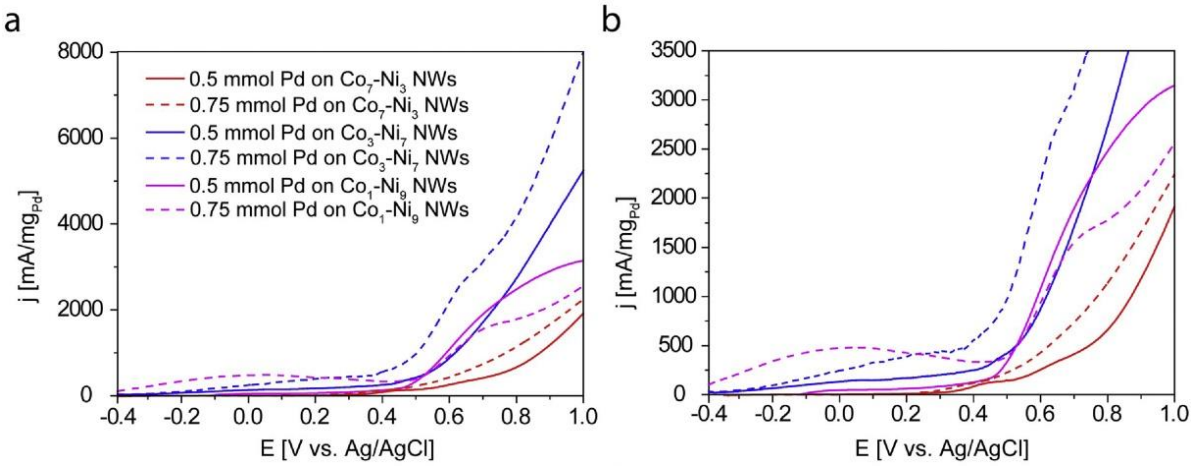

Fig. 23. (a) Comparison of the cyclic voltammograms (EOR curves) of electrocatalysts in the form of cobalt-nickel nanowires with different Co:Ni ratios decorated by Pd in argon-saturated 1.0 M NaOH + 0.5 M CH_3CH_2OH solution at a scan rate of 20 mV/s; (b) plot showing an enlargement of the data between 0 and 3500 mA/mg_{Pd}. Reproduced and modified with permission from [199]. Copyright (2022) Elsevier.

The presented work showed a strong correlation between the morphology of support nanostructure and the crystallization of noble metal. The phase composition of Co-Ni nanowires controlled the way of decoration with palladium by preferring oxidized or metallic forms of nanoparticles. As a result, the catalytic properties of the final nanocomposite could be optimized to meet requirements for highly active and durable catalytic systems for specified applications. Obtained findings unravel a part of mechanisms, which drive the deposition of palladium species on metal-based anisotropic nanomaterials and reveal new opportunities for studies in the future.

4. Conclusions and further perspective

This dissertation was focused on a nanotechnological approach for catalysis-related chemical transformations. As a main target, the application of nanowires as catalysts was explored. The introduction section highlighted the most common routes for the synthesis of such anisotropic nanostructures and their participation in catalytical studies of various chemical reactions [P1]. Literature showed how nanowires impact the modern development of catalysis, in which their contribution exhibits promising results in many fields such as organic chemistry, electrocatalysis, and photocatalysis. However, there are still countless compositions of nanowires, which are waiting for proper characterization and may find an intriguing and prosperous application in this area and beyond.

Among the synthesis of various nanowires, one of the presented works described the formation of anisotropic nanostructures from industrial wastewater [P2]. The possibility of transforming such inconvenient solutions into nanomaterials is an interesting outcome of my internship at Aalto University in Finland. Due to restricted ecologic policy in most countries around the globe, waste management is a crucial issue, which can be addressed by obtained results. Recycling heavy metals from highly acidic solutions is difficult due to its complex composition and large amounts of produced waste. On the other hand, extracted copper and nickel successfully served as a precursor solution for an environmentally-conscious synthesis of nanostructures. Those findings revealed new frontiers of waste transformation into advanced nanomaterials.

The study of catalytic properties of nanowire-based systems was covered by utilizing nickel and cobalt-nickel nanowires as support materials for highly active palladium nanoparticles [P3, P4, P5]. Those non-noble metals are perfect candidates for such tasks due to their abundant nature and inexpensive precursors used to create them. In that case, large-scale production of nanowires can be fairly easily achieved. Suzuki-Miyaura reaction was targeted as a testing ground for PdNPs/NiNWs composite due to the high importance of such reaction in organic chemistry synthesis [P3]. Among novel catalysts, nanowires are in the minority, as homogeneous complexes are mainly

studied. This creates a research niche, which presented papers should fill with new information. The proposed system successfully facilitated anisole and toluene derivatives coupling with organic phenylboronic acid derivatives under conventional heating. However, the true potential of PdNPs/NiNWs was only discovered when microwaves were used. Its application resulted in a significant improvement of catalytic properties, facilitating shorter reaction times and higher yields of synthesized biphenyls. Similar behavior was observed for the Suzuki polycondensation reaction [P4]. Microwave irradiation-generated hot spots were the main reason for higher activities, as they promoted reactions near catalytic active sites and improved mass and energy transfers. For electrocatalytic application, bimetallic nanowires containing cobalt and nickel were used [P5]. Detailed characterization of samples allowed deep analysis of the relations between morphology and catalytic performance. Despite sparse Pd concentration, studied nanomaterials exhibited promising results.

Nanowires are very interesting nanomaterials, which possess unique properties. They can find applications in many industries, however, at this stage, the main targets for them are electronic devices, while other fields of exploitation such as catalysis remain to be explored to a more satisfactory extent. Presented outcomes of long-term research confirmed the significance of nanowires in catalysis and their properties, proving that subsequent research in this area is strongly advised. Further study of the topics discussed in this dissertation should focus on expanding the scope of metallic nanowires and nanoparticles as well as their bimetallic counterparts. Additional interest should be devoted to non-noble metals such as Ni, Cu, or Fe, whose abundance and low price are major benefits for the convenient production of nanomaterials. Synergistic effects of numerous composites may reveal enhanced catalytic properties in presented fields of catalysis. Moreover, other application opportunities should be exploited to attract more attention of scientific and industrial communities. For instance, processes in the gaseous phase or plasma-enhanced synthesis should also be considered, as they could gain from the catalytic properties of such nanomaterials. The study of nanowires in catalysis is an enormous blank spot in science, which should be addressed with high priority, as those nanomaterials have the potential to revolutionize this research field.

Blibliography

1. National Nanotechnology Initiative (NNI). https://www.nano.gov/ (Accessed 12.12.2023).

2. Franke, M. E. “There is plenty of room at the bottom for innovation”: a report on “Nano2004”, the 7th International Conference on Nanostructured Materials. *Small* **1**, 22–4 (2005).

3. Taniguchi, N. On the basic concept of’nano-technology’. in *Proc. Intl. Conf. Prod. Eng. Tokyo, Part II, 1974* (1974).

4. Iijima, S. & Ichihashi, T. Single-shell carbon nanotubes of 1-nm diameter. *Nature* **363**, 603–605 (1993).

5. Iijima, S. Helical microtubules of graphitic carbon. *Nature* **354**, 56–58 (1991).

6. Sannicolo, T. *et al.* Metallic Nanowire-Based Transparent Electrodes for Next Generation Flexible Devices: a Review. *Small* **12**, 6052–6075 (2016).

7. Zhang, Y., Guo, J., Xu, D., Sun, Y. & Yan, F. One-Pot Synthesis and Purification of Ultralong Silver Nanowires for Flexible Transparent Conductive Electrodes. *ACS Appl. Mater. Interfaces* acsami.7b07146 (2017) doi:10.1021/acsami.7b07146.

8. Ravi Kumar, D. V., Woo, K. & Moon, J. Promising wet chemical strategies to synthesize Cu nanowires for emerging electronic applications. *Nanoscale* vol. 7 17195–17210 at https://doi.org/10.1039/c5nr05138j (2015).

9. Fukata, N., Oshima, T., Tsurui, T., Ito, S. & Murakami, K. Synthesis of silicon nanowires using laser ablation method and their manipulation by electron beam. *Sci. Technol. Adv. Mater.* **6**, 628–632 (2005).

10. Xu, J. *et al.* Large-Scale Synthesis of Long Crystalline Cu 2-x Se Nanowire Bundles by Water-Evaporation-Induced Self-Assembly and Their Application in Gas Sensing. *Adv. Funct. Mater.* **19**, 1759–1766 (2009).

11. Willander, M. *et al.* Zinc oxide nanowires: Controlled low temperature growth and some electrochemical and optical nano-devices. *J. Mater. Chem.* **19**, 1006–1018 (2009).

12. Li, Y., Yang, X.-Y., Rooke, J., Tendeloo, G. Van & Su, B.-L. Ultralong Cu(OH)2 and CuO nanowire bundles: PEG200-directed crystal growth for enhanced photocatalytic performance. *J. Colloid Interface Sci.* **348**, 303–312 (2010).

13. Wagner, R. S. & Ellis, W. C. Vapor-liquid-solid mechanism of single crystal growth. *Appl. Phys. Lett.* **4**, 89–90 (1964).

14. Westwater, J., Gosain, D. p., Yamauchi, K. & Usui, S. Nanoscale silicon whiskers formed by silane/gold reaction at 335 °C. *Mater. Lett.* **24**, 109–112 (1995).

15. Askey, J., Hunt, M. O., Langbein, W. & Ladak, S. Use of Two-Photon Lithography with a Negative Resist and Processing to Realise Cylindrical Magnetic Nanowires.

Nanomaterials **10**, 429 (2020).

16. Liu, S., Tok, J. B. H. & Bao, Z. Nanowire lithography: Fabricating controllable electrode gaps using Au-Ag-Au nanowires. *Nano Lett.* **5**, 1071–1076 (2005).

17. Inagaki, Y. *et al.* Selectively enhanced crystal growth of periodically arrayed ZnO nanowires by mist chemical vapor deposition and electron beam lithography. *J. Cryst. Growth* **618**, 127309 (2023).

18. McIntyre, P. C. & Fontcuberta i Morral, A. Semiconductor nanowires: to grow or not to grow? *Mater. Today Nano* **9**, 100058 (2020).

19. Juhasz, R., Elfström, N. & Linnros, J. Controlled Fabrication of Silicon Nanowires by Electron Beam Lithography and Electrochemical Size Reduction. *Nano Lett.* **5**, 275–280 (2005).

20. Mårtensson, T. *et al.* Nanowire Arrays Defined by Nanoimprint Lithography. *Nano Lett.* **4**, 699–702 (2004).

21. Yan, X.-M., Kwon, S., Contreras, A. M., Bokor, J. & Somorjai, G. A. Fabrication of Large Number Density Platinum Nanowire Arrays by Size Reduction Lithography and Nanoimprint Lithography. *Nano Lett.* **5**, 745–748 (2005).

22. Vazquez-Mena, O. *et al.* Metallic Nanowires by Full Wafer Stencil Lithography. *Nano Lett.* **8**, 3675–3682 (2008).

23. Wu, B., Kumar, A. & Pamarthy, S. High aspect ratio silicon etch: A review. *J. Appl. Phys.* **108**, (2010).

24. Khanlary, M. R., Alijarahi, S. & Reyhani, A. Growth temperature dependence of VLS-grown ultra-long ZnS nanowires prepared by CVD method. *J. Theor. Appl. Phys.* **12**, 121–126 (2018).

25. Kim, S. *et al.* Synthesis of SnO2 nanowires using thermal chemical vapor deposition with SnO powder and their application as self-powered ultraviolet photodetectors. *J. Alloys Compd.* **963**, 171265 (2023).

26. Zeng, F., Zhang, X., Wang, J., Wang, L. & Zhang, L. Large-scale growth of In 2 O 3 nanowires and their optical properties. *Nanotechnology* **15**, 596–600 (2004).

27. Morber, J. R. *et al.* PLD-Assisted VLS Growth of Aligned Ferrite Nanorods, Nanowires, and NanobeltsSynthesis, and Properties. *J. Phys. Chem. B* **110**, 21672–21679 (2006).

28. Koren, E. *et al.* Obtaining uniform dopant distributions in VLS-grown Si nanowires. *Nano Lett.* **11**, 183–187 (2011).

29. Heath, J. R. & LeGoues, F. K. A liquid solution synthesis of single crystal germanium quantum wires. *Chem. Phys. Lett.* **208**, 263–268 (1993).

30. Liu, M. *et al.* Polyacrylamide-Assisted Solvothermal Growth of Oriented Cobalt Nanowires with High Magnetic Coercivity. *J. Nanosci. Nanotechnol.* **16**, 12671–

12676 (2016).

31. Chu, Y., Wan, L., Wang, X. & Zhang, J. Synthesis and characterization of ZnO nanowires by solvothermal method and fabrication of nanowire-based ZnO nanofilms. *ICEPT-HDP 2012 Proc. - 2012 13th Int. Conf. Electron. Packag. Technol. High Density Packag.* 366–369 (2012) doi:10.1109/ICEPT-HDP.2012.6474635.

32. Xu, D., Liu, Z., Liang, J. & Qian, Y. Solvothermal synthesis of CdS nanowires in a mixed solvent of ethylenediamine and dodecanethiol. *J. Phys. Chem. B* **109**, 14344–14349 (2005).

33. Khademalrasool, M. & Farbod, M. A Simple and High Yield Solvothermal Synthesis of Uniform Silver Nanowires with Controllable Diameters. *J. Nanostructures* **5**, 415–422 (2015).

34. Bari, B. *et al.* Simple hydrothermal synthesis of very-long and thin silver nanowires and their application in high quality transparent electrodes. *J. Mater. Chem. A* **4**, 11365–11371 (2016).

35. Tiano, A. L., Koenigsmann, C., Santulli, A. C. & Wong, S. S. Solution-based synthetic strategies for one-dimensional metal-containing nanostructures. *Chem. Commun.* **46**, 8093 (2010).

36. Cushing, B. L., Kolesnichenko, V. L. & O'Connor, C. J. Recent Advances in the Liquid-Phase Syntheses of Inorganic Nanoparticles. *Chem. Rev.* **104**, 3893–3946 (2004).

37. Wulff, G. No Title. *Zeitschrift für Krist.* **34**, 449 (1901).

38. Kong, Y. Y., Pang, S. C. & Chin, S. F. Facile synthesis of nickel nanowires with controllable morphology. *Mater. Lett.* **142**, 1–3 (2015).

39. Wang, S. *et al.* Controllable synthesis of nickel nanowires and its application in high sensitivity, stretchable strain sensor for body motion sensing. *J. Mater. Chem. C* **6**, 4737–4745 (2018).

40. Wasiak, T., Przypis, L., Walczak, K. & Janas, D. Nickel Nanowires: Synthesis, Characterization and Application as Effective Catalysts for the Reduction of Nitroarenes. *Catalysts* **8**, 566 (2018).

41. Guangming, W., Dan, L., Jianxiang, Y. & Dongdong, F. Synthesis of copper nanowires via a liquid phase reduction process. *Integr. Ferroelectr.* **183**, 1–7 (2017).

42. Lin, T. Y. *et al.* In Situ Investigation of Defect-Free Copper Nanowire Growth. *Nano Lett.* **18**, 778–784 (2018).

43. Liu, Z. *et al.* Synthesis of Copper Nanowires via a Complex-Surfactant-Assisted Hydrothermal Reduction Process. *J. Phys. Chem. B* **107**, 12658–12661 (2003).

44. Yokoyama, S., Motomiya, K., Jeyadevan, B. & Tohji, K. Environmentally friendly

synthesis and formation mechanism of copper nanowires with controlled aspect ratios from aqueous solution with ascorbic acid. *J. Colloid Interface Sci.* **531**, 109–118 (2018).

45. Li, X. *et al.* Synthesis of cobalt nanowires in aqueous solution under an external magnetic field. *Beilstein J. Nanotechnol.* **7**, 990–994 (2016).

46. Balela, M. D. L., Dulin, L. M., Garcia, E. A. & Tica, M. J. H. Synthesis and Characterization of Cobalt-Nickel Nanowires Formed under External Magnetic Field. *Appl. Mech. Mater.* **799**–**800**, 120–124 (2015).

47. Sun, Y., Mayers, B., Herricks, T. & Xia, Y. Polyol synthesis of uniform silver nanowires: A plausible growth mechanism and the supporting evidence. *Nano Lett.* **3**, 955–960 (2003).

48. Yan, W., Wang, D., Diaz, L. A. & Botte, G. G. Nickel nanowires as effective catalysts for urea electro-oxidation. *Electrochim. Acta* **134**, 266–271 (2014).

49. Li, C. . *et al.* Ultrafine and uniform silicon nanowires grown with zeolites. *Chem. Phys. Lett.* **365**, 22–26 (2002).

50. Schönenberger, C. *et al.* Template Synthesis of Nanowires in Porous Polycarbonate Membranes: Electrochemistry and Morphology. *J. Phys. Chem. B* **101**, 5497–5505 (1997).

51. Lazzara, T. D., Bourret, G. R., Lennox, R. B. & van de Ven, T. G. M. Polymer Templated Synthesis of AgCN and Ag Nanowires. *Chem. Mater.* **21**, 2020–2026 (2009).

52. Cui, S., Liu, Y., Yang, Z. & Wei, X. Construction of silver nanowires on DNA template by an electrochemical technique. *Mater. Des.* **28**, 722–725 (2007).

53. Wu, Q., Zheng, N., Ding, Y. & Li, Y. Micelle-template inducing synthesis of winding ZnS nanowires. *Inorg. Chem. Commun.* **5**, 671–673 (2002).

54. Cao, H. Q. *et al.* Sol-Gel Template Synthesis of an Array of Single Crystal CdS Nanowires on a Porous Alumina Template. *Adv. Mater.* **13**, 1393–1394 (2001).

55. Hurst, S. J., Payne, E. K., Qin, L. & Mirkin, C. A. Multisegmented One-Dimensional Nanorods Prepared by Hard-Template Synthetic Methods. *Angew. Chemie Int. Ed.* **45**, 2672–2692 (2006).

56. Manzano, C. V. & Martin-Gonzalez, M. Electrodeposition of V-VI Nanowires and Their Thermoelectric Properties. *Front. Chem.* **7**, (2019).

57. Caffarena, V. da R., Capitaneo, J. L., Simão, R. A. & Guimarães, A. P. Preparation of electrodeposited cobalt nanowires. *Mater. Res.* **9**, 205–208 (2006).

58. Meier, L. A., Alvarez, A. E., García, S. G. & del Barrio, M. C. Formation of Cu and Ni Nanowires by Electrodeposition. *Procedia Mater. Sci.* **8**, 617–622 (2015).

59. Mahenderkar, N. K., Liu, Y.-C., Koza, J. A. & Switzer, J. A. Electrodeposited

Germanium Nanowires. *ACS Nano* **8**, 9524–9530 (2014).

60. Mahshid, S. S., Dolati, A., Hashemi Daryan, S., Ghorbani, M. & Ghahramaninezhad, A. Electrodeposition of Platinum Nanowires: Electrochemical Characterization. *ECS Trans.* **28**, 25–35 (2010).

61. Boughey, F. L. *et al.* Vertically aligned zinc oxide nanowires electrodeposited within porous polycarbonate templates for vibrational energy harvesting. *Nanotechnology* **27**, (2016).

62. Martín-García, L. *et al.* Multifunctional core–shell Co–SiO 2 nanowires via electrodeposition and sol–gel techniques. *RSC Adv.* **5**, 97503–97507 (2015).

63. Martín-González, M., Prieto, A. L., Gronsky, R., Sands, T. & Stacy, A. M. High-Density 40 nm Diameter Sb-Rich Bi2xSbxTe3 Nanowire Arrays. *Adv. Mater.* **15**, 1003–1006 (2003).

64. Lu, X., Wang, C. & Wei, Y. One-Dimensional Composite Nanomaterials: Synthesis by Electrospinning and Their Applications. *Small* **5**, 2349–2370 (2009).

65. Greiner, A. & Wendorff, J. H. Electrospinning: A Fascinating Method for the Preparation of Ultrathin Fibers. *Angew. Chemie Int. Ed.* **46**, 5670–5703 (2007).

66. Roduner, E. Understanding catalysis. *Chem. Soc. Rev.* **43**, 8226–8239 (2014).

67. Mąkosza, M. & Fedoryński, M. Phase Transfer Catalysis. in *Encyclopedia of Catalysis* (Wiley, 2010). doi:10.1002/0471227617.eoc170.pub2.

68. Veldsink, J. W., Bouma, M. J., Schöön, N. H. & Beenackers, A. A. C. M. Heterogeneous Hydrogenation of Vegetable Oils: A Literature Review. *Catal. Rev.* **39**, 253–318 (1997).

69. Kumar Dutta, D., Jyoti Borah, B. & Pollov Sarmah, P. Recent Advances in Metal Nanoparticles Stabilization into Nanopores of Montmorillonite and Their Catalytic Applications for Fine Chemicals Synthesis. *Catal. Rev.* **57**, 257–305 (2015).

70. Biesemans, B., De Clercq, J., Stevens, C. V., Thybaut, J. W. & Lauwaert, J. Recent advances in amine catalyzed aldol condensations. *Catal. Rev.* 1–83 (2022) doi:10.1080/01614940.2022.2048570.

71. Liu, Z., Ma, L., Zhang, J., Hongsirikarn, K. & Goodwin, J. G. Pt Alloy Electrocatalysts for Proton Exchange Membrane Fuel Cells: A Review. *Catal. Rev.* **55**, 255–288 (2013).

72. SCHNEIDER, M. & BAIKER, A. Aerogels in Catalysis. *Catal. Rev.* **37**, 515–556 (1995).

73. King, A. O. & Yasuda, N. Palladium-Catalyzed Cross-Coupling Reactions in the Synthesis of Pharmaceuticals. 205–245 (2004) doi:10.1007/b94551.

74. Emadi, R. *et al.* Applications of palladium-catalyzed C–N cross-coupling reactions

in pharmaceutical compounds. *RSC Adv.* **13**, 18715–18733 (2023).

75. Torborg, C. & Beller, M. Recent Applications of Palladium-Catalyzed Coupling Reactions in the Pharmaceutical, Agrochemical, and Fine Chemical Industries. *Adv. Synth. Catal.* **351**, 3027–3043 (2009).

76. Devendar, P., Qu, R.-Y., Kang, W.-M., He, B. & Yang, G.-F. Palladium-Catalyzed Cross-Coupling Reactions: A Powerful Tool for the Synthesis of Agrochemicals. *J. Agric. Food Chem.* **66**, 8914–8934 (2018).

77. Fuji, K., Tamba, S., Shono, K., Sugie, A. & Mori, A. Murahashi Coupling Polymerization: Nickel(II)–N-Heterocyclic Carbene Complex-Catalyzed Polycondensation of Organolithium Species of (Hetero)arenes. *J. Am. Chem. Soc.* **135**, 12208–12211 (2013).

78. Aoki, H. *et al.* Synthesis of Conjugated Polymers Containing Octafluorobiphenylene Unit via Pd-Catalyzed Cross-Dehydrogenative-Coupling Reaction. *ACS Macro Lett.* **7**, 90–94 (2018).

79. Mondal, S. Recent advancement of Ullmann-type coupling reactions in the formation of C–C bond. *ChemTexts* **2**, 1–11 (2016).

80. FANTA, P. E. The Ullmann Synthesis of Biaryls. *Synthesis (Stuttg).* **1974**, 9–21 (1974).

81. Miyaura, N., Yamada, K. & Suzuki, A. A new stereospecific cross-coupling by the palladium-catalyzed reaction of 1-alkenylboranes with 1-alkenyl or 1-alkynyl halides. *Tetrahedron Lett.* **20**, 3437–3440 (1979).

82. Tamao, K., Sumitani, K. & Kumada, M. Selective carbon-carbon bond formation by cross-coupling of Grignard reagents with organic halides. Catalysis by nickel-phosphine complexes. *J. Am. Chem. Soc.* **94**, 4374–4376 (1972).

83. Milstein, D. & Stille, J. K. Palladium-Catalyzed Coupling of Tetraorganotin Compounds with Aryl and Benzyl Halides. Synthetic Utility and Mechanism. *J. Am. Chem. Soc.* **101**, 4992–4998 (1979).

84. Xu, S., Kim, E. H., Wei, A. & Negishi, E. Pd- and Ni-catalyzed cross-coupling reactions in the synthesis of organic electronic materials. *Sci. Technol. Adv. Mater.* **15**, 044201 (2014).

85. Sonogashira, K., Tohda, Y. & Hagihara, N. A convenient synthesis of acetylenes: catalytic substitutions of acetylenic hydrogen with bromoalkenes, iodoarenes and bromopyridines. *Tetrahedron Lett.* **16**, 4467–4470 (1975).

86. Heck, R. F. Palladium-Catalyzed Vinylation of Organic Halides. in *Organic Reactions* 345–390 (Wiley, 1982). doi:10.1002/0471264180.or027.02.

87. Nelson, T. D. & Crouch, R. D. <scp>Cu</scp> , <scp>Ni</scp> , and <scp>Pd</scp> Mediated Homocoupling Reactions in Biaryl Syntheses: The <scp>U</scp> llmann Reaction. in *Organic Reactions* 265–555 (Wiley, 2004).

doi:10.1002/0471264180.or063.03.

88. Baba, S. & Negishi, E. A novel stereospecific alkenyl-alkenyl cross-coupling by a palladium- or nickel-catalyzed reaction of alkenylalanes with alkenyl halides. *J. Am. Chem. Soc.* **98**, 6729–6731 (1976).

89. Chawla, M., Kumar, R. & Siril, P. F. High catalytic activities of palladium nanowires synthesized using liquid crystal templating approach. *J. Mol. Catal. A Chem.* **423**, 126–134 (2016).

90. Lakshminarayana, B., Chakraborty, J., Satyanarayana, G. & Subrahmanyam, C. Recyclable Pd/CuFe2O4 nanowires: A highly active catalyst for C-C couplings and synthesis of benzofuran derivatives. *RSC Adv.* **8**, 21030–21039 (2018).

91. Lakshminarayana, B. *et al.* Fabrication of Pd/CuFe2O4 hybrid nanowires: A heterogeneous catalyst for Heck couplings. *New J. Chem.* **42**, 1646–1654 (2018).

92. Gao, S. *et al.* Palladium nanowires stabilized by thiol-functionalized ionic liquid: seed-mediated synthesis and heterogeneous catalyst for Sonogashira coupling reaction. *Nanotechnology* **16**, 1234–1237 (2005).

93. Wasiak, T. & Janas, D. Nanowires as a versatile catalytic platform for facilitating chemical transformations. *J. Alloys Compd.* **892**, 162158 (2022).

94. Chen, W. *et al.* C – S Cross-Coupling Reactions Catalyzed by Recyclable Core-Shell Structured Copper/ Cu 2 O Nanowires Under Ligand-Free Conditions. *J. Mol. Eng. Mater.* **03**, 1540001 (2015).

95. Nasrollahzadeh, M., Azarian, A., Ehsani, A., Sajadi, S. M. & Babaei, F. Hybrid Pd/Fe3O4 nanowires: Fabrication, characterization, optical properties and application as magnetically reusable catalyst for the synthesis of N-monosubstituted ureas under ligand-free conditions. *Mater. Res. Bull.* **55**, 168–175 (2014).

96. Hu, L. *et al.* Ultrathin platinum nanowire catalysts for direct C-N coupling of carbonyls with aromatic nitro compounds under 1 bar of hydrogen. *Chem. - A Eur. J.* **17**, 14283–14287 (2011).

97. Lv, J.-J. J. *et al.* Facile synthesis of highly active Pd-Cu nanowires catalyst through a simple wet-chemical strategy for ligand-free Suzuki cross coupling reaction. *Appl. Catal. A Gen.* **522**, 188–193 (2016).

98. Podeh, M. R. H., Sarhadi, M. & Ghoreishi, S. M. A Combined Chemical Reduction and Biological Oxidation Process for the Treatment of Textile Wastewater. *Water Qual. Res. J.* **36**, 605–617 (2001).

99. Imura, Y., Tsujimoto, K., Morita, C. & Kawai, T. Preparation and Catalytic Activity of Pd and Bimetallic Pd–Ni Nanowires. *Langmuir* **30**, 5026–5030 (2014).

100. Sun, Y., Zhang, F., Xu, L., Yin, Z. & Song, X. Roughness-controlled copper nanowires and Cu nanowires-Ag heterostructures: Synthesis and their enhanced

catalysis. *J. Mater. Chem. A* **2**, 18583–18592 (2014).

101. Sun, L. *et al.* Preparation and catalytic activity of magnetic bimetallic nickel/copper nanowires. *RSC Adv.* **7**, 17781–17787 (2017).

102. Xu, Z. *et al.* Catalytic reduction of 4-nitrophenol over graphene supported Cu@Ni bimetallic nanowires. *Mater. Chem. Phys.* **227**, 64–71 (2019).

103. Senapati, S., Srivastava, S. K., Singh, S. B. & Mishra, H. N. Magnetic Ni/Ag core-shell nanostructure from prickly Ni nanowire precursor and its catalytic and antibacterial activity. *J. Mater. Chem.* **22**, 6899–6906 (2012).

104. Sarkar, S. *et al.* Redox Transmetalation of Prickly Nickel Nanowires for Morphology Controlled Hierarchical Synthesis of Nickel/Gold Nanostructures for Enhanced Catalytic Activity and SERS Responsive Functional Material. *J. Phys. Chem. C* **115**, 1659–1673 (2011).

105. Fu, H., Yang, X., Jiang, X. & Yu, A. Bimetallic Ag-Au nanowires: Synthesis, growth mechanism, and catalytic properties. *Langmuir* **29**, 7134–7142 (2013).

106. Ezeta, A., Arce, E. M., Solorza, O., González, R. G. & Dorantes, H. Effect of the leaching of Ru-Se-Fe and Ru-Mo-Fe obtained by mechanical alloying on electrocatalytical behavior for the oxygen reduction reaction. *J. Alloys Compd.* **483**, 429–431 (2009).

107. Schulenburg, H. *et al.* 3D Imaging of catalyst support corrosion in polymer electrolyte fuel cells. *J. Phys. Chem. C* **115**, 14236–14243 (2011).

108. Choi, S. M., Kim, J. H., Jung, J. Y., Yoon, E. Y. & Kim, W. B. Pt nanowires prepared via a polymer template method: Its promise toward high Pt-loaded electrocatalysts for methanol oxidation. *Electrochim. Acta* **53**, 5804–5811 (2008).

109. Yu, L. *et al.* Cu nanowires shelled with NiFe layered double hydroxide nanosheets as bifunctional electrocatalysts for overall water splitting. *Energy Environ. Sci.* **10**, 1820–1827 (2017).

110. Anantharaj, S. *et al.* Recent Trends and Perspectives in Electrochemical Water Splitting with an Emphasis on Sulfide, Selenide, and Phosphide Catalysts of Fe, Co, and Ni: A Review. *ACS Catal.* **6**, 8069–8097 (2016).

111. Yan, Y., Xia, B. Y., Zhao, B. & Wang, X. A review on noble-metal-free bifunctional heterogeneous catalysts for overall electrochemical water splitting. *J. Mater. Chem. A* **4**, 17587–17603 (2016).

112. Shiva Kumar, S. & Himabindu, V. Hydrogen production by PEM water electrolysis – A review. *Mater. Sci. Energy Technol.* **2**, 442–454 (2019).

113. Yin, H. *et al.* Ultrathin platinum nanowires grown on single-layered nickel hydroxide with high hydrogen evolution activity. *Nat. Commun.* **6**, 1–8 (2015).

114. Guo, S. *et al.* FePt and CoPt Nanowires as Efficient Catalysts for the Oxygen

Reduction Reaction. *Angew. Chemie Int. Ed.* **52**, 3465–3468 (2013).

115. Luo, M. *et al.* Stable High-Index Faceted Pt Skin on Zigzag-Like PtFe Nanowires Enhances Oxygen Reduction Catalysis. *Adv. Mater.* **30**, 1705515 (2018).

116. K, J. *et al.* Efficient oxygen reduction catalysis by subnanometer Pt alloy nanowires. *Sci. Adv.* **3**, (2017).

117. Wang, P. *et al.* Precise tuning in platinum-nickel/nickel sulfide interface nanowires for synergistic hydrogen evolution catalysis. *Nat. Commun.* **8**, 1–9 (2017).

118. Koenigsmann, C. *et al.* Enhanced Electrocatalytic Performance of Processed, Ultrathin, Supported Pd–Pt Core–Shell Nanowire Catalysts for the Oxygen Reduction Reaction. *J. Am. Chem. Soc.* **133**, 9783–9795 (2011).

119. Huang, X., Xu, X., Luan, X. & Cheng, D. CoP nanowires coupled with CoMoP nanosheets as a highly efficient cooperative catalyst for hydrogen evolution reaction. *Nano Energy* **68**, 104332 (2020).

120. Yang, L. *et al.* Co-N-doped MoO2 nanowires as efficient electrocatalysts for the oxygen reduction reaction and hydrogen evolution reaction. *Nano Energy* **41**, 772–779 (2017).

121. Han, Y. *et al.* Facile synthesis of Ni based metal-organic frameworks wrapped MnO2 nanowires with high performance toward electrochemical oxygen evolution reaction. *Talanta* **186**, 154–161 (2018).

122. Fu, L., Yang, F., Cheng, G. & Luo, W. Ultrathin Ir nanowires as high-performance electrocatalysts for efficient water splitting in acidic media. *Nanoscale* **10**, 1892–1897 (2018).

123. Alia, S. M., Shulda, S., Ngo, C., Pylypenko, S. & Pivovar, B. S. Iridium-Based Nanowires as Highly Active, Oxygen Evolution Reaction Electrocatalysts. *ACS Catal.* **8**, 2111–2120 (2018).

124. Zhao, L. *et al.* Iron oxide embedded titania nanowires – An active and stable electrocatalyst for oxygen evolution in acidic media. *Nano Energy* **45**, 118–126 (2018).

125. Zhang, Y. *et al.* Rapid Synthesis of Cobalt Nitride Nanowires: Highly Efficient and Low-Cost Catalysts for Oxygen Evolution. *Angew. Chemie - Int. Ed.* **55**, 8670–8674 (2016).

126. Tang, C., Cheng, N., Pu, Z., Xing, W. & Sun, X. NiSe Nanowire Film Supported on Nickel Foam: An Efficient and Stable 3D Bifunctional Electrode for Full Water Splitting. *Angew. Chemie Int. Ed.* **54**, 9351–9355 (2015).

127. Guo, Y., Guo, D., Ye, F., Wang, K. & Shi, Z. Synthesis of lawn-like NiS2 nanowires on carbon fiber paper as bifunctional electrode for water splitting. *Int. J. Hydrogen Energy* **42**, 17038–17048 (2017).

128. Guo, S. *et al.* FePt and CoPt nanowires as efficient catalysts for the oxygen reduction reaction. *Angew. Chemie - Int. Ed.* **52**, 3465–3468 (2013).

129. Koenigsmann, C. *et al.* Enhanced electrocatalytic performance of processed, ultrathin, supported Pd-Pt core-shell nanowire catalysts for the oxygen reduction reaction. *J. Am. Chem. Soc.* **133**, 9783–9795 (2011).

130. Yu, L. *et al.* Cu nanowires shelled with NiFe layered double hydroxide nanosheets as bifunctional electrocatalysts for overall water splitting. *Energy Environ. Sci.* **10**, 1820–1827 (2017).

131. Wasmus, S. & Küver, A. Methanol oxidation and direct methanol fuel cells: a selective review. *J. Electroanal. Chem.* **461**, 14–31 (1999).

132. Wang, H. *et al.* Pd/Pt core–shell nanowire arrays as highly effective electrocatalysts for methanol electrooxidation in direct methanol fuel cells. *Electrochem. commun.* **10**, 1575–1578 (2008).

133. Li, H. H. *et al.* Ultrathin PtPdTe nanowires as superior catalysts for methanol electrooxidation. *Angew. Chemie - Int. Ed.* **52**, 7472–7476 (2013).

134. Shang, C., Guo, Y. & Wang, E. Facile fabrication of PdRuPt nanowire networks with tunable compositions as efficient methanol electrooxidation catalysts. *Nano Res.* **11**, 4348–4355 (2018).

135. Guo, S., Zhang, S., Sun, X. & Sun, S. Synthesis of Ultrathin FePtPd Nanowires and Their Use as Catalysts for Methanol Oxidation Reaction. *J. Am. Chem. Soc.* **133**, 15354–15357 (2011).

136. Zhang, Y., Gao, F., Wang, C., Shiraishi, Y. & Du, Y. Engineering Spiny PtFePd@PtFe/Pt Core@Multishell Nanowires with Enhanced Performance for Alcohol Electrooxidation. *ACS Appl. Mater. Interfaces* **11**, 30880–30886 (2019).

137. Li, C. *et al.* An efficient ultrathin PtFeNi Nanowire/Ionic liquid conjugate electrocatalyst. *Appl. Catal. B Environ.* **256**, 117828 (2019).

138. Zhang, C., Xu, L., Yan, Y. & Chen, J. Controlled Synthesis of Pt Nanowires with Ordered Large Mesopores for Methanol Oxidation Reaction. *Sci. Rep.* **6**, 31440 (2016).

139. Guo, S., Zhang, S., Sun, X. & Sun, S. Synthesis of Ultrathin FePtPd Nanowires and Their Use as Catalysts for Methanol Oxidation Reaction. *J. Am. Chem. Soc.* **133**, 15354–15357 (2011).

140. Pei, J. *et al.* Ultrathin Pt–Zn Nanowires: High-Performance Catalysts for Electrooxidation of Methanol and Formic Acid. *ACS Sustain. Chem. Eng.* **6**, 77–81 (2018).

141. Xiao, M. *et al.* Enhanced Catalytic Performance of Composition-Tunable PtCu Nanowire Networks for Methanol Electrooxidation. *ChemCatChem* **6**, 2825–2831 (2014).

142. Xie, L. *et al.* Cu(OH) 2 @CoCO 3 (OH) 2 · n H 2 O Core-Shell Heterostructure Nanowire Array: An Efficient 3D Anodic Catalyst for Oxygen Evolution and Methanol Electrooxidation. *Small* **13**, 1602755 (2017).

143. FUJISHIMA, A., ZHANG, X. & TRYK, D. TiO2 photocatalysis and related surface phenomena. *Surf. Sci. Rep.* **63**, 515–582 (2008).

144. Tong, H. *et al.* Nano-photocatalytic Materials: Possibilities and Challenges. *Adv. Mater.* **24**, 229–251 (2012).

145. Yang, J., Wang, D., Han, H. & Li, C. Roles of Cocatalysts in Photocatalysis and Photoelectrocatalysis. *Acc. Chem. Res.* **46**, 1900–1909 (2013).

146. Hoffmann, M. R., Martin, S. T., Choi, W. & Bahnemann, D. W. Environmental Applications of Semiconductor Photocatalysis. *Chem. Rev.* **95**, 69–96 (1995).

147. Fernández, C., Larrechi, M. S. & Callao, M. P. An analytical overview of processes for removing organic dyes from wastewater effluents. *TrAC Trends Anal. Chem.* **29**, 1202–1211 (2010).

148. Rauf, M. A. & Ashraf, S. S. Fundamental principles and application of heterogeneous photocatalytic degradation of dyes in solution. *Chemical Engineering Journal* vol. 151 10–18 at https://doi.org/10.1016/j.cej.2009.02.026 (2009).

149. Vautier, M., Guillard, C. & Herrmann, J.-M. Photocatalytic Degradation of Dyes in Water: Case Study of Indigo and of Indigo Carmine. *J. Catal.* **201**, 46–59 (2001).

150. Brahiti, N., Hadjersi, T., Amirouche, S., Menari, H. & ElKechai, O. Photocatalytic degradation of cationic and anionic dyes in water using hydrogen-terminated silicon nanowires as catalyst. *Int. J. Hydrogen Energy* **43**, 11411–11421 (2018).

151. Xue, X. *et al.* Piezo-potential enhanced photocatalytic degradation of organic dye using ZnO nanowires. *Nano Energy* **13**, 414–422 (2015).

152. Jung, H. S. *et al.* Photocatalysis using GaN nanowires. *ACS Nano* **2**, 637–642 (2008).

153. Liu, B. *et al.* Visible-light photocatalysis in Cu 2 Se nanowires with exposed {111} facets and charge separation between (111) and ($\bar{1}\bar{1}\bar{1}$) polar surfaces. *Phys. Chem. Chem. Phys.* **17**, 13280–13289 (2015).

154. Shi, H., Chen, G., Zhang, C. & Zou, Z. Polymeric g-C 3 N 4 Coupled with NaNbO 3 Nanowires toward Enhanced Photocatalytic Reduction of CO 2 into Renewable Fuel. *ACS Catal.* **4**, 3637–3643 (2014).

155. Chang, Y., Lye, M. L. & Zeng, H. C. Large-Scale Synthesis of High-Quality Ultralong Copper Nanowires. *Langmuir* **21**, 3746–3748 (2005).

156. Wasiak, T., Hannula, P.-M., Lundström, M. & Janas, D. Transformation of industrial wastewater into copper-nickel nanowire composites: straightforward

recycling of heavy metals to obtain products of high added value. *Sci. Rep.* **10**, Article 19190 (2020).

157. Daff, T. D., Saadoune, I., Lisiecki, I. & de Leeuw, N. H. Computer simulations of the effect of atomic structure and coordination on the stabilities and melting behaviour of copper surfaces and nano-particles. *Surf. Sci.* **603**, 445–454 (2009).

158. Rathmell, A. R., Bergin, S. M., Hua, Y.-L. L., Li, Z.-Y. Y. & Wiley, B. J. The Growth Mechanism of Copper Nanowires and Their Properties in Flexible, Transparent Conducting Films. *Adv. Mater.* **22**, 3558–3563 (2010).

159. Farhang, M., Akbarzadeh, A. R., Rabbani, M. & Ghadiri, A. M. A retrospective-prospective review of Suzuki–Miyaura reaction: From cross-coupling reaction to pharmaceutical industry applications. *Polyhedron* **227**, 116124 (2022).

160. Martin, R. & Buchwald, S. L. Palladium-Catalyzed Suzuki−Miyaura Cross-Coupling Reactions Employing Dialkylbiaryl Phosphine Ligands. *Acc. Chem. Res.* **41**, 1461–1473 (2008).

161. Bandaru, S. S. M. *et al.* Phosphine ligands based on the ferrocenyl platform: Advances in catalytic cross-couplings. *Coord. Chem. Rev.* **491**, 215250 (2023).

162. Gan, K. B., Zhong, R.-L., Zhang, Z.-W. & Kwong, F. Y. Atropisomeric Phosphine Ligands Bearing C–N Axial Chirality: Applications in Enantioselective Suzuki–Miyaura Cross-Coupling Towards the Assembly of Tetra-ortho-Substituted Biaryls. *J. Am. Chem. Soc.* **144**, 14864–14873 (2022).

163. Wasiak, T., Łukowiec, D., Wacławek, S., Kubacki, J. & Janas, D. Ni nanowires decorated with Pd nanoparticles as an efficient nanocatalytic system for Suzuki coupling of anisole derivatives. *Nano-Structures & Nano-Objects* **36**, 101052 (2023).

164. Zhang, Y. Q., Wei, X. W. & Yu, R. Fe3O4 nanoparticles-supported palladium-bipyridine complex: Effective catalyst for suzuki coupling reaction. *Catal. Letters* **135**, 256–262 (2010).

165. Nasrollahzadeh, M., Azarian, A., Maham, M. & Ehsani, A. Synthesis of Au/Pd bimetallic nanoparticles and their application in the Suzuki coupling reaction. *J. Ind. Eng. Chem.* **21**, 746–748 (2015).

166. Chatterjee, S. & Bhattacharya, S. K. Size-Dependent Catalytic Activity and Fate of Palladium Nanoparticles in Suzuki-Miyaura Coupling Reactions. *ACS Omega* **3**, 12905–12913 (2018).

167. Mandali, P. K. & Chand, D. K. Palladium nanoparticles catalyzed Suzuki cross-coupling reactions in ambient conditions. *Catal. Commun.* **31**, 16–20 (2013).

168. Littke, A. F., Dai, C. & Fu, G. C. Versatile Catalysts for the Suzuki Cross-Coupling of Arylboronic Acids with Aryl and Vinyl Halides and Triflates under Mild Conditions. *J. Am. Chem. Soc.* **122**, 4020–4028 (2000).

169. Mahouche Chergui, S. *et al.* Hairy carbon nanotube@Nano-Pd heterostructures: Design, characterization, and application in suzuki C-C coupling reaction. *Langmuir* **26**, 16115–16121 (2010).

170. Cheng, Y. J., Yang, S. H. & Hsu, C. S. Synthesis of conjugated polymers for organic solar cell applications. *Chem. Rev.* **109**, 5868–5923 (2009).

171. Wöhrle, D. & Meissner, D. Organic Solar Cells. *Adv. Mater.* **3**, 129–138 (1991).

172. Grimsdale, A. C., Leok Chan, K., Martin, R. E., Jokisz, P. G. & Holmes, A. B. Synthesis of Light-Emitting Conjugated Polymers for Applications in Electroluminescent Devices. *Chem. Rev.* **109**, 897–1091 (2009).

173. Burroughes, J. H. *et al.* Light-emitting diodes based on conjugated polymers. *Nature* **347**, 539–541 (1990).

174. Guo, X., Baumgarten, M. & Müllen, K. Designing π-conjugated polymers for organic electronics. *Prog. Polym. Sci.* **38**, 1832–1908 (2013).

175. Moliton, A. & Hiorns, R. C. Review of electronic and optical properties of semiconducting π-conjugated polymers: applications in optoelectronics. *Polym. Int.* **53**, 1397–1412 (2004).

176. Fong, D. & Adronov, A. Recent developments in the selective dispersion of single-walled carbon nanotubes using conjugated polymers. *Chem. Sci.* **8**, 7292–7305 (2017).

177. Nish, A., Hwang, J.-Y., Doig, J. & Nicholas, R. J. Highly selective dispersion of single-walled carbon nanotubes using aromatic polymers. *Nat. Nanotechnol.* **2**, 640–646 (2007).

178. Sudakov, I. *et al.* Chirality Dependence of Triplet Excitons in (6,5) and (7,5) Single-Wall Carbon Nanotubes Revealed by Optically Detected Magnetic Resonance. *ACS Nano* **17**, 2190–2204 (2023).

179. Dzienia, A., Just, D. & Janas, D. Solvatochromism in SWCNTs suspended by conjugated polymers in organic solvents. *Nanoscale* **15**, 9510–9524 (2023).

180. He, P. *et al.* Capillary electrophoresis of covalently functionalized single-chirality carbon nanotubes. *Electrophoresis* **38**, 1669–1677 (2017).

181. Fleurier, R., Lauret, J., Lopez, U. & Loiseau, A. Transmission Electron Microscopy and UV–vis–IR Spectroscopy Analysis of the Diameter Sorting of Carbon Nanotubes by Gradient Density Ultracentrifugation. *Adv. Funct. Mater.* **19**, 2219–2223 (2009).

182. Liu, H., Tanaka, T. & Kataura, H. Optical Isomer Separation of Single-Chirality Carbon Nanotubes Using Gel Column Chromatography. *Nano Lett.* **14**, 6237–6243 (2014).

183. Ouyang, J. *et al.* Impact of Conjugated Polymer Characteristics on the Enrichment of Single-Chirality Single-Walled Carbon Nanotubes. *ACS Appl.*

Polym. Mater. **4**, 6239–6254 (2022).

184. Wasiak, T. *et al.* PdNPs/NiNWs as a welding tool for the synthesis of polyfluorene derivatives by Suzuki polycondensation under microwave radiation. *Sci. Rep.* **14**, 2336 (2024).

185. de la Hoz, A., Díaz-Ortiz, Á. & Moreno, A. Microwaves in organic synthesis. Thermal and non-thermal microwave effects. *Chem. Soc. Rev.* **34**, 164–178 (2005).

186. Metzler, L. *et al.* High molecular weight mechanochromic spiropyran main chain copolymers via reproducible microwave-assisted Suzuki polycondensation. *Polym. Chem.* **6**, 3694–3707 (2015).

187. Miyaura, N. & Suzuki, A. Palladium-Catalyzed Cross-Coupling Reactions of Organoboron Compounds. *Chem. Rev.* **95**, 2457–2483 (1995).

188. Hassan, J., Sévignon, M., Gozzi, C., Schulz, E. & Lemaire, M. Aryl−Aryl Bond Formation One Century after the Discovery of the Ullmann Reaction. *Chem. Rev.* **102**, 1359–1470 (2002).

189. Zou, G. & Falck, J. . Suzuki–Miyaura cross-coupling of lithium n-alkylborates. *Tetrahedron Lett.* **42**, 5817–5819 (2001).

190. Krishna, A., Lunchev, A. V. & Grimsdale, A. C. Suzuki Polycondensation. in *Synthetic Methods for Conjugated Polymers and Carbon Materials* 59–95 (Wiley, 2017). doi:10.1002/9783527695959.ch2.

191. Horikoshi, S., Osawa, A., Abe, M. & Serpone, N. On the Generation of Hot-Spots by Microwave Electric and Magnetic Fields and Their Impact on a Microwave-Assisted Heterogeneous Reaction in the Presence of Metallic Pd Nanoparticles on an Activated Carbon Support. *J. Phys. Chem. C* **115**, 23030–23035 (2011).

192. Petricci, E., Risi, C., Ferlin, F., Lanari, D. & Vaccaro, L. Avoiding hot-spots in Microwave-assisted Pd/C catalysed reactions by using the biomass derived solvent γ-Valerolactone. *Sci. Rep.* **8**, 10571 (2018).

193. Horikoshi, S., Osawa, A., Sakamoto, S. & Serpone, N. Control of microwave-generated hot spots. Part V. Mechanisms of hot-spot generation and aggregation of catalyst in a microwave-assisted reaction in toluene catalyzed by Pd-loaded AC particulates. *Appl. Catal. A Gen.* **460**–**461**, 52–60 (2013).

194. Ding, J. *et al.* Enrichment of large-diameter semiconducting SWCNTs by polyfluorene extraction for high network density thin film transistors. *Nanoscale* **6**, 2328 (2014).

195. Marks-Bielska, R., Bielski, S., Pik, K. & Kurowska, K. The Importance of Renewable Energy Sources in Poland's Energy Mix. *Energies* **13**, 4624 (2020).

196. Qerimi, D., Dimitrieska, C., Vasilevska, S. & Rrecaj, A. A. Modeling of the Solar Thermal Energy Use in Urban Areas. *Civ. Eng. J.* **6**, 1349–1367 (2020).

197. Shen, S. Y., Zhao, T. S., Xu, J. B. & Li, Y. S. Synthesis of PdNi catalysts for the oxidation of ethanol in alkaline direct ethanol fuel cells. *J. Power Sources* **195**, 1001–1006 (2010).

198. Tan, J. L. *et al.* Preparation and characterization of palladium-nickel on graphene oxide support as anode catalyst for alkaline direct ethanol fuel cell. *Appl. Catal. A Gen.* **531**, 29–35 (2017).

199. Łukowiec, D. *et al.* Pd decorated Co–Ni nanowires as a highly efficient catalyst for direct ethanol fuel cells. *Int. J. Hydrogen Energy* **47**, 41279–41293 (2022).

200. Zhang, J.-W., Zhang, B. & Zhang, X. Enhanced catalytic activity of ternary NiCoPd nanocatalyst dispersed on carbon nanotubes toward methanol oxidation reaction in alkaline media. *J. Solid State Electrochem.* **21**, 447–453 (2017).

201. Jiang, Y., Lu, Y., Han, D., Zhang, Q. & Niu, L. Hollow Ag@Pd core–shell nanotubes as highly active catalysts for the electro-oxidation of formic acid. *Nanotechnology* **23**, 105609 (2012).

202. Kottayintavida, R. & Gopalan, N. K. Pd modified Ni nanowire as an efficient electro-catalyst for alcohol oxidation reaction. *Int. J. Hydrogen Energy* **45**, 8396–8404 (2020).

203. Liu, Z., Zhang, X. & Hong, L. Physical and electrochemical characterizations of nanostructured Pd/C and PdNi/C catalysts for methanol oxidation. *Electrochem. commun.* **11**, 925–928 (2009).

Academic achievements

1. Publications

1.1. T. Siudyga, M. Kapkowski, D. Janas, T. Wasiak, R. Sitko, M. Zubko, J. Szade, K. Balin, J. Klimontko, D. Lach, J. Popiel, A. Smoliński, J. Polanski, *Nano-Ru Supported on Ni Nanowires for Low-Temperature Carbon Dioxide Methanation*, Cat. 10 (2020) 513. https://doi.org/10.3390/catal10050513

1.2. [P2] T. Wasiak, P.-M. Hannula, M. Lundström, D. Janas, *Transformation of industrial wastewater into copper-nickel nanowire composites: straightforward recycling of heavy metals to obtain products of high added value*, Sci. Rep. 10 (2020) Article 19190. https://doi.org/10.1038/s41598-020-76374-x

1.3. [P5] D. Łukowiec, T. Wasiak, D. Janas, E. Drzymała, J. Depciuch, T. Tarnawski, J. Kubacki, S. Wacławek, A. Radoń, *Pd decorated Co–Ni nanowires as a highly efficient catalyst for direct ethanol fuel cells*, Int. J. Hydrogen Energy (2021). https://doi.org/10.1016/j.ijhydene.2021.11.177

1.4. [P1] T. Wasiak, D. Janas, *Nanowires as a versatile catalytic platform for facilitating chemical transformations*, J. Alloys Compd. 892 (2022) 162158. https://doi.org/10.1016/j.jallcom.2021.162158

1.5. P. Taborowska, T. Wasiak, M. Sahlman, M. Lundström, D. Janas, *Carbon Nanotube-Based Thermoelectric Modules Enhanced by ZnO Nanowires*, Mater. 2022, Vol. 15, Page 1924. 15 (2022) 1924. https://doi.org/10.3390/ma15051924

1.6. [P3] T. Wasiak, D. Łukowiec, S. Wacławek, J. Kubacki, D. Janas, *Ni nanowires decorated with Pd nanoparticles as an efficient nanocatalytic system for Suzuki coupling of anisole derivatives*, Nano-Structures & Nano-Objects 36 (2023) 101052. https://doi.org/10.1016/j.nanoso.2023.101052

1.7. [P4] T. Wasiak, D. Just, A. Dzienia, D. Łukowiec, S. Wacławek, A. Mielańczyk, S. Kodan, A. Bansal, R. Chandra, D. Janas, *PdNPs/NiNWs as a welding tool for the synthesis of polyfluorene derivatives by Suzuki polycondensation under microwave radiation*, Sci. Rep. 14 (2024) 2336. https://doi.org/ 10.1038/s41598-024-52795-w

2. Research projects

04.2018 – 12.2021

Co-Investigator in the project "Nanohybr1Ds: Hybrids composed of carbon nanotubes and metallic nanowires for harvesting energy from waste heat" (LIDER/0001/L8/16/NCBR/2017), LIDER 9, Principal Investigator: Dawid Janas Ph.D. DSc, source of funding: National Center of Research and Development, amount of funding: 1 199 995 zł.

3. Pending patents

T. Wasiak, D. Janas, *Method of producing hybrid materials and carbon nanomaterials*, application no: P.435987 (submission date: 16.11.2020)

4. Internships

4.1. 05.08 – 30.08.2019: Aalto University in Espoo (Finland)

4.2. 11.03 – 08.04.2023: Indian Institute of Technology in Roorkee (India)

5. Conferences

5.1. InterNanoPoland, Katowice, Poland, 14-15.04.2021, Poster: *Copper-nickel nanocomposites originating from industrial wastes as a modern approach in recycling*, T. Wasiak, P-M. Hannula, M. Lundström, D. Janas

5.2. International Conference on the Science and Application of Nanotubes and Low-Dimensional Materials NT21, Houston, USA, 6-11.06.2021, Poster: *Complex industrial waste solutions as an alternative source of metal ions for copper-nickel nanocomposites,* T. Wasiak, P-M. Hannula, M. Lundström, D. Janas

5.3. IEEE NAP, Bratislava, Slovakia, 10-15.09.2023, Poster: *Nickel nanowires decorated with palladium nanoparticles as powerful catalysts facilitating synthesis of polyfluorene derivatives by Suzuki polycondensation*, T. Wasiak, D. Just, A. Dzienia, D. Łukowiec, S. Wacławek, A. Mielańczyk, D. Janas